Finite element method for the reconstruction of a time-dependent heat source in isotropic thermoelasticity systems of type-III

Karel Van Bockstal and Liviu Marin

Abstract. The isotropic thermoelasticity system of type-III, describing both the mechanical and the thermal behaviours of a body occupying a bounded domain with a Lipschitz boundary, is considered. The displacement vector and either the normal heat flux or the temperature are prescribed on the boundary. Both the theoretical and the numerical reconstructions of a time-dependent heat source from the knowledge of an additional weighted integral measurement of the temperature are investigated. It is showed that the appropriate type of measurement depends on the thermal boundary condition available, whilst the existence and uniqueness of a weak solution for exact data is also proved. For each of the two inverse source problems investigated herein, a numerical algorithm is also proposed and the convergence of these numerical schemes for exact data is proved. Four numerical examples with noisy measurements are implemented using the finite element method and thoroughly investigated to validate the convergence and stability of the proposed algorithms.

Mathematics Subject Classification (2010). MSC 74F05; MSC 35R30; MSC 65M32; MSC 65M60.

Keywords. isotropic thermoelasticity; inverse problem; finite element.

1. Introduction

1.1. Literature review

The problem of transmission of heat flow in rigid or elastic materials has attracted considerable attention from numerous researchers. Many important fields of application, such as casting, metal forming, manufacturing processes, structural models, etc., give rise to coupled thermomechanical problems. Variational principles for the coupled problems of thermoelasticity (the change in size and shape of a solid object as the temperature of that object fluctuates) were firstly stated by Biot [4]. These interactions between the changes in the shape of an object and the fluctuations in the temperature are modeled by the so-called thermoelasticity systems that consist of two coupled partial differential equations (PDEs), namely a parabolic PDE (heat transfer equation) for the temperature and a hyperbolic system of PDEs for the displacement vector. Numerous papers have been published following Biot's principle, see e.g. [8, 12] and the references therein. Various variational principles have been formulated [34] based on Gurtin's method of convolution [16]. Numerous studies that are devoted to the theoretical and numerical analysis of problems associated with novel models in thermoelasticity, have appeared in the literature [3, 6, 33, 46, 23].

The heat flow in thermoelastic bodies was described by Green and Naghdi [13] using a general entropy balance. The characterization of material response for such thermal phenomena is referred to

.

as type-I, type-II and type-III thermoelasticity according to Green and Naghdi [13]. The type-I thermoelasticity becomes identical to the classical heat conduction theory (Fourier's law) via linearization. However, this theory has the following shortcoming: a thermal disturbance at one point of the body is instantly felt everywhere, i.e. infinite speed of propagation. This fact is physically unacceptable for materials with memory and is overcome by accounting for memory effects in the models for type-II and type-III thermoelasticity. More precisely, type-II and type-III thermoelasticity theories allow for the propagation of thermoelastic disturbances at a finite speed. It should be mentioned that the heat conduction is independent of the present values of the temperature gradient for type-II thermoelasticity as compared to type-III thermoelasticity.

Inverse problems in thermoelasticity are characterized by the partial or complete lack of at least one of the following conditions:

(i) the boundary and/or initial conditions (i.e. boundary and/or initial data reconstruction problems);
(ii) the material properties (i.e. coefficient identification problems);
(iii) the geometry of the domain of interest (i.e. inverse geometric problems);
(iv) the magnitudes and locations of any possible sources of stress, deformation, or heat inside or on the boundary of the domain (i.e. inverse source or load reconstruction problems).

It is well-known that most of these inverse problems are ill-posed in the sense of Hadamard [17], i.e. small errors in the measurements may significantly be amplified in the resulting solution. Therefore, such inverse problems are more difficult to solve than direct problems and special methods should be designed for obtaining an accurate, stable and physically meaningful solution to such inverse problems.

The inverse problems in thermoelasticity addressed so far in the literature are mainly related to boundary data reconstruction, identification of material parameters, shape optimization problems and detection of flaws, i.e. items (i)–(iii), see [9, 11, 29, 24, 31, 45, 10, 32, 21, 20]. However, over the past decades, several studies have been devoted to inverse source or load reconstruction problems, i.e. item (iv), related to classical thermoelasticity [2, 43, 41, 40, 44, 42]. An inverse space-dependent heat source problem for type-I thermoelasticity has been studied by Bellassoued and Yamamoto [2]. Wu and Liu [43] have investigated the reconstruction of a space-dependent vector source in type-II thermoelasticity. In these papers, the uniqueness of a solution to the inverse source problem was proved by employing Carleman estimates, however a numerical scheme for calculations was not provided. Van Bockstal and Slodička [41] have provided a stable iterative algorithm for the recovery of a space-dependent vector source, for all types of isotropic thermoelasticity, from an additional measurement at the final time. Later, Van Bockstal and Marin [40] extended this result to anisotropic thermoelasticity by considering various assumptions on the convolution kernel k. Wu et al. [44] have investigated the uniqueness and stability of a spatially varying thermal kernel function in a thermoelastic system of type-III by means of a Carleman estimate. Van Bockstal and Slodička [42] investigated the reconstruction of the source $h(t)$ from the measurement (3) with $\omega = 1$ for the one-dimensional isotropic thermoelasticity system of type-III. The results presented in [42] will be discussed in detail in Section 2.

1.2. Mathematical formulation of the problem

We consider an isotropic homogeneous thermoelastic body occupying an open and bounded domain $\Omega \subset \mathbb{R}^d$ with a Lipschitz continuous boundary Γ, where $d \in \mathbb{N}$ is the dimension of the space where the problem is posed, usually $d \in \{1, 2, 3\}$. Let $Q_T := \Omega \times (0, T)$ and $\Sigma_T := \Gamma \times (0, T)$, where $T > 0$ is a given final time. The convolution product of a kernel k and a function θ is denoted by

$$(k * \theta)(\mathbf{x}, t) := \int_0^t k(t - s)\theta(\mathbf{x}, s)\mathrm{d}s, \quad (\mathbf{x}, t) \in Q_T.$$

In the sequel, the following isotropic thermoelasticity system of type-III, describing both the elastic and the thermal behaviours in Ω, is considered

$$\begin{cases} \varrho\partial_{tt}\mathbf{u}(\mathbf{x},t) - \mu\Delta\mathbf{u}(\mathbf{x},t) - (\lambda+\mu)\nabla\left(\nabla\cdot\mathbf{u}\right)(\mathbf{x},t) + \beta\nabla\theta(\mathbf{x},t) = \mathbf{p}(\mathbf{x},t), & (\mathbf{x},t)\in Q_T, \\ \varrho C_s\partial_t\theta(\mathbf{x},t) - \kappa\Delta\theta(\mathbf{x},t) - (k*\Delta\theta)(\mathbf{x},t) + T_0\beta\nabla\cdot\partial_t\mathbf{u}(\mathbf{x},t) = h(t)f(\mathbf{x}) + F(\mathbf{x},t), & (\mathbf{x},t)\in Q_T, \\ \mathbf{u}(\mathbf{x},t) = \mathbf{0}, & (\mathbf{x},t)\in \Sigma_T, \\ -\kappa\nabla\theta(\mathbf{x},t)\cdot\boldsymbol{\nu}(\mathbf{x}) = g \quad \text{or} \quad \theta = 0, & (\mathbf{x},t)\in\Sigma_T, \end{cases} \tag{1}$$

together with the initial conditions

$$\mathbf{u}(\mathbf{x},0) = \overline{\mathbf{u}}_0(\mathbf{x}), \quad \partial_t\mathbf{u}(\mathbf{x},0) = \overline{\mathbf{u}}_1(\mathbf{x}), \quad \theta(\mathbf{x},0) = \overline{\theta}_0(\mathbf{x}), \quad \mathbf{x}\in\Omega. \tag{2}$$

Here, the heat source $h(t)$ is assumed to be unknown and depends solely on the time variable, whilst the load source $\mathbf{p}$ and the heat source F are assumed to be given. Furthermore, $\mathbf{u} = (u_1,\dots,u_d)^{\mathsf{T}}$ and θ denote the displacement and the temperature difference from the reference value $T_0 > 0$ (in Kelvin), respectively, of the thermoelastic material at point $\mathbf{x}$ and time t, with the mention that the reference temperature corresponds to the undeformed and unstressed state of the material. We suppose that either the normal heat flux g is known at every point of the boundary Γ (note that $\boldsymbol{\nu}(\mathbf{x})$ denotes the outward unit normal vector at the point $\mathbf{x}\in\Gamma$) or that the temperature is known at the boundary. Moreover, we assume that the displacement field is prescribed at the boundary.

The constant coefficients $\lambda > 0$ and $\mu > 0$ are the so-called Lamé parameters. These quantities may be expressed in terms of the shear modulus $G > 0$ and Poisson's ratio $\nu \in (0, 0.5)$ as

$$\lambda = \frac{2\nu G}{1-2\nu} \quad \text{and} \quad \mu = G.$$

The coefficients κ, ρ and C_s denote the thermal conductivity, the mass density ρ and the specific heat C_s of the material. The coupling parameter $\beta > 0$ is defined as

$$\beta = \alpha_T(3\lambda + 2\mu) = 2\alpha_T G\frac{1+\nu}{1-2\nu},$$

where $\alpha_T > 0$ is the coefficient of linear expansion of the thermoelastic material. The goal of this paper is to investigate how the heat source $h(t)$ can be theoretically and numerically determined from the knowledge of the additional integral measurement

$$m(t) \coloneqq \int_\Omega \omega(\mathbf{x})\theta(\mathbf{x},t)\ \mathrm{d}\mathbf{x}, \quad t\in[0,T], \tag{3}$$

with the weight function ω be specified later. We will show that a different choice for the boundary condition of the temperature leads to different conditions on ω. This will be explained in detail in Section 2, where the inverse source problem is reformulated as a direct coupled problem. The existence and uniqueness of a solution by means of Rothe's method - in the case of a Neumann boundary condition - is studied in Section 3, whilst the case of a Dirichlet boundary condition is discussed in Section 4. Finally, Section 5 concerns the numerical implementation of the algorithms proposed in the previous sections.

We conclude this section with the notations used herein.

Remark 1.1 (Notations). *We denote by $(\cdot,\cdot)$ the standard inner product in $\mathrm{L}^2(\Omega)$ and by $\|\cdot\|$ its induced norm. Let X be an abstract Banach space endowed with the norm $\|\cdot\|_X$. Assume that $k\in\mathbb{N}\cup\{0\}$. The set of k-times continuously differentiable functions $w : [0,T]\to X$, equipped with the usual norm*

$$\sum_{j=0}^{k}\max_{t\in[0,T]}\|w^{(j)}(t)\|_X,$$

is denoted by $\mathrm{C}^k([0,T],X)$. The space $\mathrm{L}^p((0,T),X)$ is endowed with the norm $\left(\int_0^T\|\cdot\|_X^p\right)^{1/p}$ with $p>1$. The symbol X^* stands for the dual space of X. Finally, C,ε and C_ε denote generic positive constants depending only on a priori known quantities, where ε is small and $C_\varepsilon = C\left(\varepsilon^{-1}\right)$ is large.

Remark 1.2. *The recovery of a time-dependent source in isotropic heat conduction from an integral over-determination condition – more precisely, an average temperature over a (sub)domain – was studied by Cannon and Lin* [5] *and Prilepko et al.* [35]*. In particular, the local-in-time existence of a sufficiently smooth solution under a compatibility condition on the measurement and/or data was proven. The same inverse source problem was investigated by Ismailov et al.* [22] *and Hazanee et al.* [18] *for the 1D heat equation considering nonlocal boundary and integral over-determination conditions. The existence, uniqueness and continuous dependence on the data of the solution were shown for some regularity and consistency conditions on the data. In the multidimensional case, Grimmonprez and Slodička* [15] *and Slodička* [38] *have shown the global-in-time existence of a unique solution for exact data considering an additional integral measurement of the solution over the entire domain and its surface, respectively, provided that a compatibility condition on the data was satisfied. Moreover, a numerical scheme, based on the backward Euler method, for computing an approximate solution to this problem, has also been proposed. The approach proposed herein remains valid and hence the existence of a solution to the inverse problem, for exact data, can also be obtained without imposing any restrictive compatibility conditions on the data via the weighted integral measurement.*

2. Methodology: Reformulation of the ISP as a direct problem

As already mentioned, the reconstruction of the unknown source h from the measurement (3) with $\omega = 1$ for the one-dimensional isotropic thermoelasticity system of type-III was obtained by using a decoupling technique based on Rothe's method, see [42]. This technique starts off by employing a transformation of the variational formulation of the inverse problem with the unknowns $\mathbf{u}, \theta$ and h into a variational problem in which the unknown h is written in terms of the unknowns $\mathbf{u}$ and θ. The expression for h contains the term $\int_0^L \theta''$, see Eq. (3) in [42]. The existence and uniqueness of a solution were proved by taking advantage of the one-dimensional setting and the choice of the boundary conditions ($u' = \theta = 0$ on Γ), see [42]. However, the approach followed in [42] in the case of Dirichlet boundary condition for θ does not seem possible to be extended to the multi-dimensional case since the term $\int_\Omega \Delta\theta$ in the expression for h cannot be controlled. Herein, we consider the measurement (3) with $\omega \neq 1$ and investigate the conditions on ω that enable us to prove the global in time existence of a unique solution. The main idea is to transfer the derivatives from $\mathbf{u}$ and θ to function ω. We also investigate the influence of the choice of boundary condition for θ on the analysis by considering, in addition, the Neumann boundary condition for θ. Moreover, we consider the homogeneous Dirichlet boundary condition for $\mathbf{u}$ instead of condition $u' = 0$ on Γ assumed in [42]. Finally, we mention that a similar idea was adopted by Grimmonprez et al. [14] for the reconstruction of a solely time-dependent load in a simply supported non-homogeneous Euler-Bernoulli beam (i.e. a fourth-order hyperbolic problem in the one-dimensional setting).

First, we derive an expression for the unknown source function h in terms of the unknown functions $\mathbf{u}$ and θ, and the data in case of the Neumann boundary condition for θ. Using the measurement (3) and considering the Neumann boundary condition for θ, we multiply the PDE for the temperature in system (1) by $\omega \in \mathrm{H}^1(\Omega)$ and then integrate the result over the domain Ω. By applying Green's theorem, we obtain

$$\begin{aligned} h(t) = \Big[&\rho C_s m'(t) + \kappa \left(\nabla\theta(t), \nabla\omega\right) + (g(t), \omega)_\Gamma + ((k * \nabla\theta)(t), \nabla\omega) \\ &+ \frac{1}{\kappa}\left((k*g)(t), \omega\right)_\Gamma - \beta T_0 \left(\partial_t \mathbf{u}(t), \nabla\omega\right) - (F(t), \omega)\Big] \Big/ (f, \omega), \quad \omega \in \mathrm{H}^1(\Omega), \end{aligned} \tag{4}$$

where the following assumption was made

$$(f, \omega) = \int_\Omega f(\mathbf{x})\omega(\mathbf{x}) \ \mathrm{d}\mathbf{x} \neq 0.$$

By using Green's formulas, the following variational formulation in case of the Neumann boundary condition for the temperature is obtained:

Find $(\mathbf{u}(t), \theta(t)) \in \mathbf{H}_0^1(\Omega) \times \mathrm{H}^1(\Omega)$, where $\partial_t \mathbf{u}(t) \in \mathbf{L}^2(\Omega)$, $\partial_{tt}\mathbf{u}(t) \in \mathbf{H}_0^1(\Omega)^*$ and $\partial_t \theta(t) \in \mathrm{H}^1(\Omega)^*$, such that

$$\rho\langle \partial_{tt}\mathbf{u}(t), \boldsymbol{\varphi}\rangle + \mu\,(\nabla \mathbf{u}(t), \nabla \boldsymbol{\varphi}) + (\lambda+\mu)\,(\nabla\cdot \mathbf{u}(t), \nabla\cdot\boldsymbol{\varphi}) + \beta\,(\nabla\theta(t), \boldsymbol{\varphi}) = (\mathbf{p}(t), \boldsymbol{\varphi}) \tag{5}$$

$$\begin{aligned} \rho C_s\langle \partial_t \theta(t), \psi\rangle + \kappa\,(\nabla\theta(t), \nabla\psi) + ((k*\nabla\theta)(t), \nabla\psi) - T_0\beta\,(\partial_t\mathbf{u}(t), \nabla\psi) \\ = h(t)\,(f,\psi) + (F(t),\psi) - (g(t),\psi)_\Gamma - \frac{1}{\kappa}\,((k*g)(t),\psi)_\Gamma\,, \end{aligned} \tag{6}$$

where $h(t)$ is given by (4), for a.a. $t\in(0,T)$ and any $(\boldsymbol{\varphi}, \psi) \in \mathbf{H}_0^1(\Omega)\times \mathrm{H}^1(\Omega)$.

We note that in case of the Neumann condition for θ, we may take $\omega = 1$, i.e. $m(t) = \int_\Omega \theta(\mathbf{x}, t)\ \mathrm{d}\mathbf{x}$, however when considering the homogeneous Dirichlet boundary condition for the temperature, $\omega = 0$ on Γ is required. Otherwise, the boundary term $(\nabla\theta\cdot\boldsymbol{\nu}, \omega)_\Gamma$ needs to be handled, which does not seem to be possible with the present approach. The expression for h in the case of the homogeneous Dirichlet boundary condition for θ becomes

$$\begin{aligned} h(t) = [\rho C_s m'(t) + \kappa\,(\nabla\theta(t), \nabla\omega) + ((k*\nabla\theta)(t), \nabla\omega) \\ -\beta T_0\,(\partial_t\mathbf{u}(t), \nabla\omega) - (F(t),\omega)]\,/(f,\omega), \quad \omega\in \mathrm{H}_0^1(\Omega), \end{aligned} \tag{7}$$

where the difference lies in the absence of two boundary terms in comparison with (4). In this case, the variational formulation is given by:

Find $(\mathbf{u}(t), \theta(t)) \in \mathbf{H}_0^1(\Omega) \times \mathrm{H}_0^1(\Omega)$, where $\partial_t \mathbf{u}(t) \in \mathbf{L}^2(\Omega)$, $\partial_{tt}\mathbf{u}(t) \in \mathbf{H}_0^1(\Omega)^*$ and $\partial_t \theta(t) \in \mathrm{H}_0^1(\Omega)^*$, such that

$$\rho\langle \partial_{tt}\mathbf{u}(t), \boldsymbol{\varphi}\rangle + \mu\,(\nabla \mathbf{u}(t), \nabla \boldsymbol{\varphi}) + (\lambda+\mu)\,(\nabla\cdot \mathbf{u}(t), \nabla\cdot\boldsymbol{\varphi}) + \beta\,(\nabla\theta(t), \boldsymbol{\varphi}) = (\mathbf{p}(t), \boldsymbol{\varphi}) \tag{8}$$

$$\begin{aligned} \rho C_s\langle \partial_t \theta(t), \psi\rangle + \kappa\,(\nabla\theta(t), \nabla\psi) + ((k*\nabla\theta)(t), \nabla\psi) \\ - T_0\beta\,(\partial_t\mathbf{u}(t), \nabla\psi) = h(t)\,(f,\psi) + (F(t),\psi)\,, \end{aligned} \tag{9}$$

where $h(t)$ is given by (7), for a.a. $t\in(0,T)$ and any $(\boldsymbol{\varphi}, \psi) \in \mathbf{H}_0^1(\Omega)\times \mathrm{H}_0^1(\Omega)$.

The existence of a unique solution to problem (4)–(6) is studied in the Section 3, whilst problem (7)–(9) is briefly discussed in Section 4.

3. Existence of a unique solution: Neumann boundary condition for the temperature

Rothe's method, i.e. semidiscretization in time [25], is applied to address the existence of a solution to the variational problem (4)–(6). Firstly, the time interval $[0,T]$ is divided into $n\in\mathbb{N}$ equidistant subintervals $[t_{i-1}, t_i]$, $i = \overline{1,n}$, hence $t_i = i\tau$, $i=\overline{0,n}$. The time step is denoted by $\tau = T/n < 1$. The backward Euler method is used to approximate the time derivatives at every time step, i.e. for any function z consider

$$z_i \approx z(t_i), \quad \partial_t z(t_i) \approx \delta z_i = \frac{z_i - z_{i-1}}{\tau} \ \text{ and }\ \partial_{tt} z(t_i) \approx \delta^2 z_i = \frac{z_i - z_{i-1}}{\tau^2} - \frac{\delta z_{i-1}}{\tau}.$$

Moreover, $(k*z)(\mathbf{x}, t_i)$, $i=\overline{1,n}$, is approximated as

$$(k*z)(\mathbf{x}, t_i) \approx \sum_{l=1}^{i} k_l z_{i-l}(\mathbf{x})\tau, \quad i=\overline{1,n}.$$

Note that in these approximations only the values of the temperature at previous time steps are used. Hence we may propose the following linear recurrent scheme to approximate the original problem (4)–(6) for any $(\boldsymbol{\varphi},\psi)\in \mathbf{H}_0^1(\Omega)\times \mathrm{H}^1(\Omega)$ and $i=\overline{1,n}$:

$$\rho\left(\delta^2\mathbf{u}_i,\boldsymbol{\varphi}\right)+\mu\left(\nabla\mathbf{u}_i,\nabla\boldsymbol{\varphi}\right)+(\lambda+\mu)\left(\nabla\cdot\mathbf{u}_i,\nabla\cdot\boldsymbol{\varphi}\right)+\beta\left(\nabla\theta_i,\boldsymbol{\varphi}\right)=\left(\mathbf{p}_i,\boldsymbol{\varphi}\right), \tag{10}$$

$$\begin{aligned}\rho C_s\left(\delta\theta_i,\psi\right)+\kappa\left(\nabla\theta_i,\nabla\psi\right)-T_0\beta\left(\delta\mathbf{u}_i,\nabla\psi\right)&=h_i\left(f,\psi\right)\\ &+\left(F_i,\psi\right)-\left(g_i,\psi\right)_\Gamma-\left(\sum_{l=1}^{i}k_l\nabla\theta_{i-l}\tau,\nabla\psi\right)-\frac{1}{\kappa}\left(\sum_{l=1}^{i}k_lg_{i-l}\tau,\psi\right)_\Gamma,\end{aligned} \tag{11}$$

where

$$\begin{aligned}h_i=\Bigg[\rho C_sm_i'+\kappa\left(\nabla\theta_{i-1},\nabla\omega\right)+\left(g_i,\omega\right)_\Gamma+\left(\sum_{l=1}^{i}k_l\nabla\theta_{i-l}\tau,\nabla\omega\right)\\ +\frac{1}{\kappa}\left(\sum_{l=1}^{i}k_lg_{i-l}\tau,\omega\right)_\Gamma-\beta T_0\left(\delta\mathbf{u}_{i-1},\nabla\omega\right)-\left(F_i,\omega\right)\Bigg]/(f,\omega).\end{aligned} \tag{12}$$

For a given $i\in\overline{1,n}$, we first determine h_i from relation (12) and then solve the coupled problem (10)–(11). The existence of a unique solution at every time step is proved in the following lemma.

Lemma 3.1. *Assume that $\overline{\mathbf{u}}_0,\overline{\mathbf{u}}_1\in\mathbf{L}^2(\Omega)$, $\overline{\theta}_0\in\mathrm{H}^1(\Omega)$, $f\in\mathrm{L}^2(\Omega)$ with $\int_\Omega f(\mathbf{x})\ \mathrm{d}\mathbf{x}\neq 0$, $k\in \mathrm{C}([0,T])$, $m\in\mathrm{C}^1([0,T])$, $F\in\mathrm{L}^\infty\left((0,T),\mathrm{H}^1(\Omega)\right)$, $\mathbf{p}\in\mathrm{L}^\infty\left((0,T),\mathbf{H}^1(\Omega)\right)$ and $g\in\mathrm{L}^\infty\left((0,T),\mathrm{L}^2(\Gamma)\right)$. Then, for any $i\in\overline{1,n}$, there exists a unique triplet $(\mathbf{u}_i,\theta_i,h_i)\in\mathbf{H}_0^1(\Omega)\times\mathrm{H}^1(\Omega)\times\mathbb{R}$ that solves (10)–(12).*

Proof. From relation (12), it follows that $h_i\in\mathbb{R}$ if $\mathbf{u}_l\in\mathbf{L}^2(\Omega)$ and $\theta_l\in\mathrm{L}^2(\Omega)$, for $l=\overline{0,i-1}$. Problem (10)–(11) is equivalent to solving

$$a\left(\begin{pmatrix}\mathbf{u}_i\\ \theta_i\end{pmatrix},\begin{pmatrix}\boldsymbol{\varphi}\\ \psi\end{pmatrix}\right)=\widetilde{F}_i\begin{pmatrix}\boldsymbol{\varphi}\\ \psi\end{pmatrix},\quad i=\overline{1,n},\quad \text{with}\quad \mathbf{u}_0=\overline{\mathbf{u}}_0,\quad \delta\mathbf{u}_0=\overline{\mathbf{u}}_1,\quad \theta_0=\overline{\theta}_0,$$

where $a:\left(\mathbf{H}_0^1(\Omega)\times\mathrm{H}^1(\Omega)\right)^2\to\mathbb{R}$ and $\widetilde{F}_i:\mathbf{H}_0^1(\Omega)\times\mathrm{H}^1(\Omega)\to\mathbb{R}$ are defined as

$$a\left(\begin{pmatrix}\mathbf{u}_i\\ \theta_i\end{pmatrix},\begin{pmatrix}\boldsymbol{\varphi}\\ \psi\end{pmatrix}\right):=\frac{T_0}{\tau}L_1+L_2,\quad \widetilde{F}_i\begin{pmatrix}\boldsymbol{\varphi}\\ \psi\end{pmatrix}:=\frac{T_0}{\tau}R_1+R_2,$$

with

$$\begin{aligned}L_1&:=\frac{\rho}{\tau^2}\left(\mathbf{u}_i,\boldsymbol{\varphi}\right)+\mu\left(\nabla\mathbf{u}_i,\nabla\boldsymbol{\varphi}\right)+(\lambda+\mu)\left(\nabla\cdot\mathbf{u}_i,\nabla\cdot\boldsymbol{\varphi}\right)+\beta\left(\nabla\theta_i,\boldsymbol{\varphi}\right)\\ &=\left(\mathbf{p}_i,\boldsymbol{\varphi}\right)+\frac{\rho}{\tau^2}\left(\mathbf{u}_{i-1},\boldsymbol{\varphi}\right)+\frac{\rho}{\tau}\left(\delta\mathbf{u}_{i-1},\boldsymbol{\varphi}\right)=:R_1,\end{aligned} \tag{13}$$

$$\begin{aligned}L_2&:=\frac{\rho C_s}{\tau}\left(\theta_i,\psi\right)+\kappa\left(\nabla\theta_i,\nabla\psi\right)-\frac{T_0\beta}{\tau}\left(\mathbf{u}_i,\nabla\psi\right)\\ &=h_i\left(f,\psi\right)+\left(F_i,\psi\right)-\left(g_i,\psi\right)_\Gamma-\left(\sum_{l=1}^{i}k_l\nabla\theta_{i-l}\tau,\nabla\psi\right)\\ &\quad-\frac{1}{\kappa}\left(\sum_{l=1}^{i}k_lg_{i-l}\tau,\psi\right)_\Gamma+\frac{\rho C_s}{\tau}\left(\theta_{i-1},\psi\right)-\frac{T_0\beta}{\tau}\left(\mathbf{u}_{i-1},\nabla\psi\right)=:R_2.\end{aligned} \tag{14}$$

The norm in $\mathbf{H}_0^1(\Omega)\times\mathrm{H}^1(\Omega)$ is given by $\left\|(\mathbf{u}\ \theta)^\mathsf{T}\right\|^2=\|\nabla\mathbf{u}\|^2+\|\theta\|^2_{\mathrm{H}^1(\Omega)}$. The bilinear form a is coercive and continuous on $\mathbf{H}_0^1(\Omega)\times\mathrm{H}^1(\Omega)$ since the coupling term cancels out according to the definition of a. Moreover, $\widetilde{F}_i\in\left(\mathbf{H}_0^1(\Omega)\times\mathrm{H}^1(\Omega)\right)^*$ if $\mathbf{u}_{i-1},\ \delta\mathbf{u}_{i-1}\in\mathbf{L}^2(\Omega)$, $\theta_{i-1}\in\mathrm{L}^2(\Omega)$ and $\nabla\theta_l\in\mathrm{L}^2(\Omega)$ for $l=\overline{0,i-1}$. The Lax-Milgram lemma yields the existence and uniqueness of a solution $(\mathbf{u}_i,\theta_i)\in$

$\mathbf{H}_0^1(\Omega) \times \mathrm{H}^1(\Omega)$, $i \in \overline{1,n}$, to problem (13)–(14) and, equivalently, to problem (10)–(11), provided that $\overline{\mathbf{u}}_0$, $\overline{\mathbf{u}}_1 \in \mathbf{L}^2(\Omega)$ and $\overline{\theta}_0 \in \mathrm{H}^1(\Omega)$. $\square$

Next, we derive *a priori* estimates in the following two lemmas, which serve as uniform bounds to prove the convergence of the scheme (10)–(12).

Lemma 3.2. *Let the assumptions of Lemma 3.1 be fulfilled and, in addition, assume that* $\overline{\mathbf{u}}_0 \in \mathbf{H}_0^1(\Omega)$. *Then there exist* $C > 0$ *and* $\tau_0 > 0$ *such that for any* $0 < \tau < \tau_0$, *the following relation holds*

$$\begin{aligned}\|\delta \mathbf{u}_j\|^2 + \sum_{i=1}^{j} \|\delta \mathbf{u}_i - \delta \mathbf{u}_{i-1}\|^2 + \|\nabla \mathbf{u}_j\|^2 + \|\nabla \cdot \mathbf{u}_j\|^2 \\ + \sum_{i=1}^{j} \|\nabla \mathbf{u}_i - \nabla \mathbf{u}_{i-1}\|^2 + \sum_{i=1}^{j} \|\nabla \cdot \mathbf{u}_i - \nabla \cdot \mathbf{u}_{i-1}\|^2 \\ + \|\theta_j\|^2 + \sum_{i=1}^{j} \|\theta_i - \theta_{i-1}\|^2 + \sum_{i=1}^{j} \|\nabla \theta_i\|^2 \tau \leqslant C, \quad j = \overline{1,n}, \quad (15)\end{aligned}$$

and

$$\sum_{i=1}^{j} |h_i|^2 \tau \leqslant C.$$

Proof. We set $\boldsymbol{\varphi} = \delta \mathbf{u}_i \tau$ and $\psi = \theta_i \tau / T_0$ in equations (10)–(11) and sum up these equations for $i = \overline{1,j}$ with $j = \overline{1,n}$. By summing up the two resulting equations, the coupling term cancels out and this yields

$$\begin{aligned}\rho \sum_{i=1}^{j} \left(\delta^2 \mathbf{u}_i, \delta \mathbf{u}_i\right) \tau + \mu \sum_{i=1}^{j} \left(\nabla \mathbf{u}_i, \nabla \delta \mathbf{u}_i\right) \tau + (\lambda + \mu) \sum_{i=1}^{j} \left(\nabla \cdot \mathbf{u}_i, \nabla \cdot \delta \mathbf{u}_i\right) \tau \\ + \frac{\rho C_s}{T_0} \sum_{i=1}^{j} \left(\delta \theta_i, \theta_i\right) \tau + \frac{\kappa}{T_0} \sum_{i=1}^{j} \left(\nabla \theta_i, \nabla \theta_i\right) \tau = \frac{1}{T_0} \sum_{i=1}^{j} h_i \left(f, \theta_i\right) \tau \\ + \sum_{i=1}^{j} \left(\mathbf{p}_i, \delta \mathbf{u}_i\right) \tau + \frac{1}{T_0} \sum_{i=1}^{j} \left(F_i, \theta_i\right) \tau - \frac{1}{T_0} \sum_{i=1}^{j} \left(g_i, \theta_i\right)_\Gamma \tau \\ - \frac{1}{T_0} \sum_{i=1}^{j} \left(\sum_{l=1}^{i} k_l \nabla \theta_{i-l} \tau, \nabla \theta_i\right) \tau - \frac{1}{T_0 \kappa} \sum_{i=1}^{j} \left(\sum_{l=1}^{i} k_l g_{i-l} \tau, \theta_i\right)_\Gamma \tau. \quad (16)\end{aligned}$$

We use Abel's summation rule for the first four terms on the left-hand side (LHS) of equation (16) and obtain

$$\begin{aligned}2 \sum_{i=1}^{j} \left(\delta^2 \mathbf{u}_i, \delta \mathbf{u}_i\right) \tau &= \|\delta \mathbf{u}_j\|^2 - \|\overline{\mathbf{u}}_1\|^2 + \sum_{i=1}^{j} \|\delta \mathbf{u}_i - \delta \mathbf{u}_{i-1}\|^2, \\ 2 \sum_{i=1}^{j} \left(\nabla \mathbf{u}_i, \nabla \delta \mathbf{u}_i\right) \tau &= \|\nabla \mathbf{u}_j\|^2 - \|\nabla \overline{\mathbf{u}}_0\|^2 + \sum_{i=1}^{j} \|\nabla \mathbf{u}_i - \nabla \mathbf{u}_{i-1}\|^2, \\ 2 \sum_{i=1}^{j} \left(\nabla \cdot \mathbf{u}_i, \nabla \cdot \delta \mathbf{u}_i\right) \tau &= \|\nabla \cdot \mathbf{u}_j\|^2 - \|\nabla \cdot \overline{\mathbf{u}}_0\|^2 + \sum_{i=1}^{j} \|\nabla \cdot \mathbf{u}_i - \nabla \cdot \mathbf{u}_{i-1}\|^2, \\ 2 \sum_{i=1}^{j} \left(\delta \theta_i, \theta_i\right) \tau &= \|\theta_j\|^2 - \left\|\overline{\theta}_0\right\|^2 + \sum_{i=1}^{j} \|\theta_i - \theta_{i-1}\|^2.\end{aligned}$$

Using the properties of $\mathbf{p}$ and F, it follows that

$$\left|\sum_{i=1}^{j}\left(\mathbf{p}_i,\delta\mathbf{u}_i\right)\tau+\frac{1}{T_0}\sum_{i=1}^{j}\left(F_i,\theta_i\right)\tau\right|\leqslant C\left(1+\sum_{i=1}^{j}\left\|\theta_i\right\|^2\tau+\sum_{i=1}^{j}\left\|\delta\mathbf{u}_i\right\|^2\tau\right).$$

For the last three terms on the right-hand side (RHS) of equation (16), by using the ε-Young and Nečas inequalities, we obtain

$$\begin{aligned}
\left|\sum_{i=1}^{j}\left(g_i,\theta_i\right)_\Gamma\tau\right| &\leqslant C+C\sum_{i=1}^{j}\left\|\theta_i\right\|_\Gamma^2\tau\\
&\leqslant C+C_\varepsilon\sum_{i=1}^{j}\left\|\theta_i\right\|^2\tau+\varepsilon\sum_{i=1}^{j}\left\|\nabla\theta_i\right\|^2\tau,\\
\left|\sum_{i=1}^{j}\left(\sum_{l=1}^{i}k_l\nabla\theta_{i-l}\tau,\nabla\theta_i\right)\tau\right| &\leqslant C_\varepsilon\sum_{i=1}^{j}\left(\sum_{l=0}^{i-1}\left\|\nabla\theta_l\right\|^2\tau\right)\tau+\varepsilon\sum_{i=1}^{j}\left\|\nabla\theta_i\right\|^2\tau,\\
\left|\sum_{i=1}^{j}\left(\sum_{l=1}^{i}k_l g_{i-l}\tau,\theta_i\right)_\Gamma\tau\right| &\leqslant C+C_\varepsilon\sum_{i=1}^{j}\left\|\theta_i\right\|^2\tau+\varepsilon\sum_{i=1}^{j}\left\|\nabla\theta_i\right\|^2\tau.
\end{aligned}$$

We still need to estimate the first term on the RHS of equation (16). From relation (12), we obtain that

$$|h_i|\leqslant C\left(1+\left\|\nabla\theta_{i-1}\right\|+\sum_{l=0}^{i-1}\left\|\nabla\theta_l\right\|\tau+\left\|\delta\mathbf{u}_{i-1}\right\|\right) \tag{17}$$

and, therefore,

$$\begin{aligned}
\left|\frac{1}{T_0}\sum_{i=1}^{j}h_i\left(f,\theta_i\right)\tau\right| &\leqslant \varepsilon\sum_{i=1}^{j}h_i^2\tau+C_\varepsilon\sum_{i=1}^{j}\left\|\theta_i\right\|^2\tau\\
&\leqslant \varepsilon\left(1+\sum_{l=0}^{j-1}\left\|\nabla\theta_l\right\|^2\tau+\sum_{l=0}^{j-1}\left\|\delta\mathbf{u}_l\right\|^2\tau\right)+C_\varepsilon\sum_{i=0}^{j}\left\|\theta_i\right\|^2\tau.
\end{aligned}$$

Then, we collect all estimates above and we fix $\varepsilon>0$ sufficiently small and apply Grönwall's lemma to conclude the first estimate. The second estimate follows from relation (17). □

Corollary 3.1. *Let the assumptions of Lemma 3.2 be fulfilled. Then there exists $C>0$ such that the following relations hold*

$$\sum_{i=1}^{j}\left\|\delta^2\mathbf{u}_i\right\|_{\mathbf{H}_0^1(\Omega)^*}^2\tau\leqslant C \quad \textit{and} \quad \sum_{i=1}^{j}\left\|\delta\theta_i\right\|_{\mathrm{H}^1(\Omega)^*}^2\tau\leqslant C,\quad j=\overline{1,n}. \tag{18}$$

Next, we introduce the following piecewise linear in time functions $\mathbf{U}_n,\mathbf{V}_n:[0,T]\to\mathrm{L}^2(\Omega)$.

$$\begin{aligned}
&\mathbf{U}_n(0)=\overline{\mathbf{u}}_0,\\
&\mathbf{U}_n(t)=\mathbf{u}_{i-1}+(t-t_{i-1})\delta\mathbf{u}_i,\qquad t\in(t_{i-1},t_i],\quad i=\overline{1,n};\\
&\mathbf{V}_n(0)=\overline{\mathbf{u}}_1,\\
&\mathbf{V}_n(t)=\delta\mathbf{u}_{i-1}+(t-t_{i-1})\delta^2\mathbf{u}_i,\quad t\in(t_{i-1},t_i],\quad i=\overline{1,n};
\end{aligned}$$

and the piecewise constant in time functions $\overline{\mathbf{U}}_n, \widetilde{\mathbf{U}}_n, \overline{\mathbf{V}}_n, \widetilde{\mathbf{V}}_n : [0,T] \to \mathrm{L}^2(\Omega)$

$$\begin{array}{lll} \overline{\mathbf{U}}_n(0) = \overline{\mathbf{u}}_0, & \overline{\mathbf{U}}_n(t) = \mathbf{u}_i, & t \in (t_{i-1}, t_i], \quad i = \overline{1,n}; \\ \overline{\mathbf{V}}_n(0) = \overline{\mathbf{u}}_1, & \overline{\mathbf{V}}_n(t) = \delta\mathbf{u}_i, & t \in (t_{i-1}, t_i], \quad i = \overline{1,n}; \\ \widetilde{\mathbf{U}}_n(t) = \overline{\mathbf{u}}_0, & & t \in [0,\tau], \\ \widetilde{\mathbf{U}}_n(t) = \overline{\mathbf{U}}_n(t-\tau), & & t \in (t_{i-1}, t_i], \quad i = \overline{2,n}; \\ \widetilde{\mathbf{V}}_n(t) = \overline{\mathbf{u}}_1, & & t \in [0,\tau], \\ \widetilde{\mathbf{V}}_n(t) = \overline{\mathbf{V}}_n(t-\tau), & & t \in (t_{i-1}, t_i], \quad i = \overline{2,n}. \end{array}$$

Analogously, we define Θ_n, $\overline{\Theta}_n$, $\widetilde{\Theta}_n$, $\overline{m'}_n$, $\overline{k}_n$, $\overline{g}_n$, $\overline{\mathbf{p}}_n$, $\overline{F}_n$ and $\overline{h}_n$. We also introduce the notations $\lceil\cdot\rceil_\tau$ and $\lfloor\cdot\rfloor_\tau$ defined as $\lceil t\rceil_\tau = i$ and $\lfloor t\rfloor_\tau = i-1$ for $t \in (t_{i-1}, t_i]$, respectively. Using these so-called *Rothe's functions*, the variational formulation (10)–(12) may be rewritten, for a.a. $t \in [0,T]$, as

$$\rho\left(\partial_t \mathbf{V}_n(t), \boldsymbol{\varphi}\right) + \mu\left(\nabla\overline{\mathbf{U}}_n(t), \nabla\boldsymbol{\varphi}\right) + (\lambda+\mu)\left(\nabla\cdot\overline{\mathbf{U}}_n(t), \nabla\cdot\boldsymbol{\varphi}\right) + \beta\left(\nabla\overline{\Theta}_n(t), \boldsymbol{\varphi}\right) = \left(\overline{\mathbf{p}}_n(t), \boldsymbol{\varphi}\right), \quad (19)$$

$$\begin{aligned} \rho C_s\left(\partial_t\Theta_n(t), \psi\right) + \kappa\left(\nabla\overline{\Theta}_n(t), \nabla\psi\right) - T_0\beta\left(\overline{\mathbf{V}}_n(t), \nabla\psi\right) = \overline{h}_n(t)\left(f, \psi\right) + \left(\overline{F}_n(t), \psi\right) \\ - \left(\overline{g}_n(t), \psi\right)_\Gamma - \left(\sum_{l=1}^{\lceil t\rceil_\tau} \overline{k}_n(t_l)\nabla\overline{\Theta}_n(t-t_l)\tau, \nabla\psi\right) - \frac{1}{\kappa}\left(\sum_{l=1}^{\lceil t\rceil_\tau} \overline{k}_n(t_l)\overline{g}_n(t_i-t_l)\tau, \psi\right)_\Gamma, \quad (20) \end{aligned}$$

where

$$\begin{aligned} \overline{h}_n(t) = \Bigg[\rho C_s \overline{m'}_n(t) + \kappa\left(\nabla\widetilde{\Theta}_n(t), \nabla\omega\right) + \left(\overline{g}_n(t), \omega\right)_\Gamma \\ + \left(\sum_{l=1}^{\lceil t\rceil_\tau} \overline{k}_n(t_l)\nabla\overline{\Theta}_n(t-t_l)\tau, \nabla\omega\right) + \frac{1}{\kappa}\left(\sum_{l=1}^{\lceil t\rceil_\tau} \overline{k}_n(t)\overline{g}_n(t-t_l)\tau, \omega\right)_\Gamma \\ -\beta T_0\left(\widetilde{\mathbf{V}}_n(t), \nabla\omega\right) - \left(\overline{F}_n(t), \omega\right)\Bigg] / (f, \omega). \quad (21) \end{aligned}$$

Theorem 3.1 (Existence and uniqueness: Neumann boundary condition). *Assume that* $\overline{\mathbf{u}}_0 \in \mathbf{H}_0^1(\Omega)$, $\overline{\mathbf{u}}_1 \in \mathbf{L}^2(\Omega)$, $\overline{\theta}_0 \in \mathrm{H}^1(\Omega)$, $f \in \mathrm{L}^2(\Omega)$ *with* $\int_\Omega f(\mathbf{x}) \, \mathrm{d}\mathbf{x} \neq 0$, $m \in \mathrm{C}^1([0,T])$, $F \in \mathrm{L}^\infty\left((0,T), \mathrm{H}^1(\Omega)\right)$, $\mathbf{p} \in \mathrm{L}^\infty\left((0,T), \mathbf{H}^1(\Omega)\right)$ *and* $g \in \mathrm{L}^\infty\left((0,T), \mathrm{L}^2(\Gamma)\right)$. *Then there exists a unique triplet* $(\mathbf{u}, \theta, h)$ *that solves problem* (4)–(6) *such that*

- $\mathbf{u} \in \mathrm{C}\left([0,T], \mathbf{L}^2(\Omega)\right) \cap \mathrm{L}^2\left((0,T), \mathbf{H}_0^1(\Omega)\right)$,
  $\partial_t\mathbf{u} \in \mathrm{L}^2\left((0,T), \mathbf{L}^2(\Omega)\right) \cap \mathrm{C}\left([0,T], \mathbf{H}_0^1(\Omega)^*\right)$, $\partial_{tt}\mathbf{u} \in \mathrm{L}^2\left((0,T), \mathbf{H}_0^1(\Omega)^*\right)$;
- $\theta \in \mathrm{C}\left([0,T], \mathbf{L}^2(\Omega)\right) \cap \mathrm{L}^2\left((0,T), \mathrm{H}^1(\Omega)\right)$, $\partial_t\theta \in \mathrm{L}^2\left((0,T), \mathrm{H}^1(\Omega)^*\right)$;
- $h \in \mathrm{L}^2(0,T)$.

Proof. The proof relies on a compactness argument. It follows, from the Rellich-Kondrachov theorem [7, Theorem 6.6-3], that

$$\mathbf{H}_0^1(\Omega) \hookrightarrow\hookrightarrow \mathrm{L}^2(\Omega) \hookrightarrow\hookrightarrow \mathbf{H}_0^1(\Omega)^*.$$

Lemma 3.2 implies that

$$\max_{t\in[0,T]}\left\{\left\|\overline{\mathbf{U}}_n(t)\right\|^2_{\mathbf{H}_0^1(\Omega)} + \left\|\partial_t\mathbf{U}_n(t)\right\|^2\right\} \leqslant C.$$

Hence the conditions from [25, Lemma 1.3.13] are satisfied and, therefore, there exist a function $\mathbf{u} \in \mathrm{C}\left([0,T], \mathbf{L}^2(\Omega)\right) \cap \mathrm{L}^\infty\left((0,T), \mathbf{H}_0^1(\Omega)\right)$ and a subsequence $\{\mathbf{U}_{n_l}\}_{l\in\mathbb{N}}$ of $\{\mathbf{U}_n\}_{n\in\mathbb{N}}$ such that

$$\begin{cases} \mathbf{U}_{n_l} \to \mathbf{u} & \text{in } \mathrm{C}\left([0,T], \mathbf{L}^2(\Omega)\right), \\ \mathbf{U}_{n_l}(t) \rightharpoonup \mathbf{u}(t) & \text{in } \mathbf{H}_0^1(\Omega), \text{ for all } t \in [0,T], \\ \overline{\mathbf{U}}_{n_l}(t) \rightharpoonup \mathbf{u}(t) & \text{in } \mathbf{H}_0^1(\Omega), \text{ for all } t \in [0,T], \\ \partial_t\mathbf{U}_{n_l} \rightharpoonup \partial_t\mathbf{u} & \text{in } \mathrm{L}^2\left((0,T), \mathbf{L}^2(\Omega)\right). \end{cases}$$

Moreover, from Corollary 3.1 and the reflexivity of space $\mathrm{L}^2\left((0,T),\mathbf{H}_0^1(\Omega)^*\right)$, for a subsequence (yet again, indexed by n_l), it follows that

$$\partial_t \mathbf{V}_{n_l} \rightharpoonup \partial_{tt}\mathbf{u} \quad \text{in } \mathrm{L}^2\left((0,T),\mathbf{H}_0^1(\Omega)^*\right).$$

From Lemma 3.2 and Corollary 3.1, it follows that

$$\int_0^T \|\Theta_{n_l}(t)\|_{\mathrm{H}^1(\Omega)}^2 \,\mathrm{d}t + \int_0^T \|\partial_t\Theta_{n_l}(t)\|_{\mathrm{H}^1(\Omega)^*}^2 \,\mathrm{d}t \leqslant C.$$

The generalized Aubin-Lions lemma [39, Lemma 2.12.4] implies the existence of a function $\theta \in \mathrm{C}\left([0,T],\mathrm{L}^2(\Omega)\right)$ and a subsequence $\{\Theta_{n_{l_k}}\}_{k\in\mathbb{N}}$ of $\{\Theta_n\}_{n\in\mathbb{N}}$ (denoted by the same symbol) such that

$$\begin{cases} \Theta_{n_l} \to \theta & \text{in } \mathrm{L}^2\left((0,T),\mathrm{L}^2(\Omega)\right), \\ \Theta_{n_l} \rightharpoonup \theta & \text{in } \mathrm{L}^2\left((0,T),\mathrm{H}^1(\Omega)\right), \\ \partial_t\Theta_{n_l} \rightharpoonup \partial_t\theta & \text{in } \mathrm{L}^2\left((0,T),\mathrm{H}^1(\Omega)^*\right). \end{cases}$$

Applying Lemma 3.2, we obtain that

$$\int_0^T \left\|\mathbf{U}_{n_l}(t) - \overline{\mathbf{U}}_{n_l}(t)\right\|_{\mathbf{H}_0^1(\Omega)}^2 \mathrm{d}t + \int_0^T \left\|\overline{\mathbf{U}}_{n_l}(t) - \widetilde{\mathbf{U}}_{n_l}(t)\right\|_{\mathbf{H}_0^1(\Omega)}^2 \mathrm{d}t \\ + \int_0^T \left\|\Theta_{n_l}(t) - \overline{\Theta}_{n_l}(t)\right\|^2 \mathrm{d}t + \int_0^T \left\|\overline{\Theta}_{n_l}(t) - \widetilde{\Theta}_{n_l}(t)\right\|^2 \mathrm{d}t \leqslant C\tau_{n_l},$$

i.e. $\{\mathbf{U}_{n_l}\}$, $\{\widetilde{\mathbf{U}}_{n_l}\}$ and $\{\overline{\mathbf{U}}_{n_l}\}$ have the same limit $\mathbf{u}$ in $\mathrm{L}^2\left((0,T),\mathbf{H}_0^1(\Omega)\right)$, whilst $\{\Theta_{n_l}\}$, $\{\widetilde{\Theta}_{n_l}\}$ and $\{\overline{\Theta}_{n_l}\}$ have the same limit θ in $\mathrm{L}^2\left((0,T),\mathrm{L}^2(\Omega)\right)$. Therefore, Lemma 3.2 and the reflexivity of space $\mathrm{L}^2\left((0,T),\mathrm{H}^1(\Omega)\right)$ imply that

$$\overline{\Theta}_{n_l}, \widetilde{\Theta}_{n_l} \rightharpoonup \theta \quad \text{in} \quad \mathrm{L}^2\left((0,T),\mathrm{H}^1(\Omega)\right).$$

Note that $\overline{\mathbf{V}}_n = \partial_t \mathbf{U}_n$ and

$$\int_0^T \left\|\overline{\mathbf{V}}_{n_l}(t) - \widetilde{\mathbf{V}}_{n_l}(t)\right\|^2 \mathrm{d}t \leqslant C\tau_{n_l},$$

that is

$$\overline{\mathbf{V}}_n, \widetilde{\mathbf{V}}_{n_l} \rightharpoonup \partial_t\mathbf{u} \quad \text{in} \quad \mathrm{L}^2\left((0,T),\mathbf{L}^2(\Omega)\right).$$

Moreover, from the reflexivity of space $\mathrm{L}^2\left((0,T),\mathrm{L}^2(\Omega)\right)$, it follows, in the sense of a subsequence indexed by n_l, that

$$\overline{h}_{n_l} \rightharpoonup h \quad \text{in} \quad \mathrm{L}^2\left((0,T),\mathrm{L}^2(\Omega)\right).$$

Therefore, for all $\eta \in (0,T)$, the following relation holds

$$\int_0^\eta \overline{h}_{n_l}(t)\,\mathrm{d}t \to \int_0^\eta h(t)\,\mathrm{d}t \quad \text{as} \quad l \to \infty.$$

By using Lemma 3.2, we obtain that

$$\left\|\sum_{l=1}^{\lceil t\rceil_{\tau_{n_l}}} \overline{k}_{n_l}(t_l)\overline{g}_{n_l}(t_i - t_l)\tau_{n_l} - (\overline{k}_{n_l} * \overline{g}_{n_l})(t)\right\|_{\mathrm{L}^2(\Gamma)} \\ = \left\|\int_t^{\tau_{n_l}\lceil t\rceil_{\tau_{n_l}}} \overline{k}_{n_l}(s)\overline{g}_{n_l}(t-s)\ \mathrm{d}s\right\|_{\mathrm{L}^2(\Gamma)} \leqslant C\tau_{n_l},$$

for $t \in (0,T)$ and the following relation holds

$$\left\| \int_0^\eta \sum_{l=1}^{\lceil t \rceil_{\tau_{n_l}}} \overline{k}_{n_l}(t_l) \left(\nabla\overline{\Theta}_{n_l}(t-t_l), \nabla\psi\right) \tau \, \mathrm{d}t - \int_0^\eta (\overline{k}_{n_l} * (\nabla\overline{\Theta}_{n_l}, \nabla\psi))(t) \, \mathrm{d}t \right\|$$
$$= \left\| \int_0^\eta \left(\int_t^{\tau_{n_l}\lceil t \rceil_{\tau_{n_l}}} \overline{k}_{n_l}(t-s) \left(\nabla\overline{\Theta}_{n_l}(s), \nabla\psi\right) \, \mathrm{d}s \right) \mathrm{d}t \right\| \leqslant C\sqrt{\tau_{n_l}}.$$

for any $\eta \in (0,T)$ and $\psi \in \mathrm{H}^1(\Omega)$. As far as the data are concerned, it should be mentioned that $\left|\overline{g}_{n_l} - g\right| \to 0$ a.e. on Σ_T, $\overline{\mathbf{p}}_{n_l} \to \mathbf{p}$ a.e. in Q_T, $\overline{F}_{n_l} \to F$ a.e. in Q_T, $\overline{k}_{n_l} \to k$ and $\overline{m'}_{n_l} \to m'$ in $(0,T)$ as $l \to \infty$.

Finally, the existence of a solution can be proved. We integrate relations (19)–(21) for the resulting subsequence in time over $(0,\eta) \subset (0,T)$ and pass to the limit as $\tau_{n_l} \to 0$ using the previous convergence results. Then, we differentiate the result with respect to the time variable to arrive at relations (4)–(6). The convergence of Rothe's functions towards the weak solution has been shown for a subsequence. However, taking into account the uniqueness of a solution, which we will show next, the entire Rothe's sequence converges towards the solution.

We next prove the uniqueness of a solution by contradiction. Consequently, we assume there exist two solutions $(\mathbf{u}_1, \theta_1, h_1)$ and $(\mathbf{u}_2, \theta_2, h_2)$ to problem (4)–(6) and will show that their differences $\mathbf{u} := \mathbf{u}_1 - \mathbf{u}_2$, $\theta := \theta_1 - \theta_2$ and $h := h_1 - h_2$, respectively, are a.e. equal to zero. Note that $\mathbf{u}(\cdot,0) = 0$, $\partial_t\mathbf{u}(\cdot,0) = 0$ and $\theta(\cdot,0) = 0$ in Ω. Moreover, $g = 0$ on Σ_T, $\mathbf{p} = \mathbf{0}$ in Q_T, $F = 0$ in Q_T and $m = 0$ in $[0,T]$. We first integrate relations (4)–(6) in time over $(0,\eta) \subset (0,T)$ since $\partial_t\mathbf{u}$ cannot be taken directly as a test function in (4) due to the fact that $\partial_t u(t) \notin \mathbf{H}^1_0(\Omega)$ under the present assumptions on the data. We obtain that the triplet $(\mathbf{u}, \theta, h)$ satisfies the following relations

$$\rho\left(\partial_t\mathbf{u}(\eta), \boldsymbol{\varphi}\right) + \mu\left(\int_0^\eta \nabla\mathbf{u}(t)\,\mathrm{d}t, \nabla\boldsymbol{\varphi}\right) + (\lambda+\mu)\left(\int_0^\eta \nabla\cdot\mathbf{u}(t)\,\mathrm{d}t, \nabla\cdot\boldsymbol{\varphi}\right)$$
$$+ \beta\left(\int_0^\eta \nabla\theta(t)\,\mathrm{d}t, \boldsymbol{\varphi}\right) = 0, \quad \boldsymbol{\varphi} \in \mathbf{H}^1_0(\Omega), \quad (22)$$

$$\rho C_s\left(\theta(\eta), \psi\right) + \kappa\left(\int_0^\eta \nabla\theta(t)\,\mathrm{d}t, \nabla\psi\right) + \left(\int_0^\eta (k*\nabla\theta)(t)\,\mathrm{d}t, \nabla\psi\right)$$
$$- T_0\beta\left(\mathbf{u}(\eta), \nabla\psi\right) = (f,\psi)\int_0^\eta h(t)\,\mathrm{d}t, \quad \psi \in \mathrm{H}^1(\Omega), \quad (23)$$

$$(f,\omega)\int_0^\eta h(t)\,\mathrm{d}t = \kappa\left(\int_0^\eta \nabla\theta(t)\,\mathrm{d}t, \nabla\omega\right) + \left(\int_0^\eta (k*\nabla\theta)(t)\,\mathrm{d}t, \nabla\omega\right) - \beta T_0\left(\mathbf{u}(\eta), \nabla\omega\right). \quad (24)$$

Take $\boldsymbol{\varphi} = \mathbf{u}(\eta)$ and $\psi = \dfrac{1}{T_0}\displaystyle\int_0^\eta \theta(t)\,\mathrm{d}t$ in relations (22) and (23), respectively, integrate the resulting equations in time over $\eta \in (0,\xi) \subset (0,T)$ and add them up. Since the coupling terms cancel out, it follows that

$$\frac{\rho}{2}\left\|\mathbf{u}(\xi)\right\|^2 + \frac{\mu}{2}\left\|\int_0^\xi \nabla\mathbf{u}(t)\,\mathrm{d}t\right\|^2 + \frac{\lambda+\mu}{2}\left\|\int_0^\xi \nabla\cdot\mathbf{u}(t)\,\mathrm{d}t\right\|^2$$
$$+ \frac{\rho C_s}{2T_0}\left\|\int_0^\xi \theta(t)\,\mathrm{d}t\right\|^2 + \frac{\kappa}{T_0}\int_0^\xi\left\|\int_0^\eta \nabla\theta(t)\,\mathrm{d}t\right\|^2\mathrm{d}\eta + \frac{1}{T_0}\int_0^\xi\left(\int_0^\eta (k*\nabla\theta)(t)\,\mathrm{d}t, \int_0^\eta \nabla\theta(t)\,\mathrm{d}t\right)\mathrm{d}\eta$$
$$= \frac{1}{T_0}\int_0^\xi\left(f, \int_0^\eta \theta(t)\,\mathrm{d}t\right)\left(\int_0^\eta h(t)\,\mathrm{d}t\right)\mathrm{d}\eta. \quad (25)$$

By using $\int_0^\eta (k*\nabla\theta)(t)\,\mathrm{d}t = \left(k * \int_0^{\bullet}\nabla\theta\right)(\eta)$, we obtain for the last term on the LHS of equation (25)

$$
\left|\int_0^\xi \left(\int_0^\eta (k*\nabla\theta)(t)\,\mathrm{d}t, \int_0^\eta \nabla\theta(t)\,\mathrm{d}t\right)\mathrm{d}\eta\right|
\leqslant C_\varepsilon \int_0^\xi \left(\int_0^\eta \left\|\int_0^t \nabla\theta(s)\ \mathrm{d}s\right\|^2 \mathrm{d}t\right)\mathrm{d}\eta + \varepsilon\int_0^\xi \left\|\int_0^\eta \nabla\theta(t)\,\mathrm{d}t\right\|^2 \mathrm{d}\eta.
$$

From relation (24), it follows that

$$
\left|\int_0^\eta h(t)\,\mathrm{d}t\right| \leqslant C\left(\left\|\int_0^\eta \nabla\theta(t)\,\mathrm{d}t\right\| + \left\|\left(k*\int_0^\bullet \nabla\theta\right)(\eta)\right\| + \|\mathbf{u}(\eta)\|\right).
$$

Therefore, using the ε-Young inequality, for the second term on the RHS of relation (25) we obtain

$$
\left|\int_0^\xi \left(f, \int_0^\eta \theta(t)\,\mathrm{d}t\right)\left(\int_0^\eta h(t)\,\mathrm{d}t\right)\mathrm{d}\eta\right|
\leqslant C_\varepsilon \int_0^\xi \left\|\int_0^\eta \theta(t)\,\mathrm{d}t\right\|^2 \mathrm{d}\eta + \varepsilon\int_0^\xi \left\|\int_0^\eta \nabla\theta(t)\,\mathrm{d}t\right\|^2 \mathrm{d}\eta + \varepsilon\int_0^\xi \|\mathbf{u}(\eta)\|^2\,\mathrm{d}\eta.
$$

By accounting for the above results, equation (25) yields

$$
\begin{aligned}
&\frac{\rho}{2}\|\mathbf{u}(\xi)\|^2 + \frac{\mu}{2}\left\|\int_0^\xi \nabla\mathbf{u}(t)\,\mathrm{d}t\right\|^2 + \frac{\lambda+\mu}{2}\left\|\int_0^\xi \nabla\cdot\mathbf{u}(t)\,\mathrm{d}t\right\|^2 \\
&\quad + \frac{\rho C_s}{2T_0}\left\|\int_0^\xi \theta(t)\,\mathrm{d}t\right\|^2 + \left(\frac{\kappa}{T_0} - \varepsilon\right)\int_0^\xi \left\|\int_0^\eta \nabla\theta(t)\,\mathrm{d}t\right\|^2 \mathrm{d}\eta \\
&\quad \leqslant C_\varepsilon \int_0^\xi \left(\int_0^\eta \left\|\int_0^t \nabla\theta(s)\ \mathrm{d}s\right\|^2 \mathrm{d}t\right)\mathrm{d}\eta \\
&\qquad + C_\varepsilon \int_0^\xi \left\|\int_0^t \theta(s)\ \mathrm{d}s\right\|^2 \mathrm{d}t + C_\varepsilon \int_0^\xi \|\mathbf{u}(\eta)\|^2\,\mathrm{d}\eta.
\end{aligned}
$$

Next, we fix $\varepsilon > 0$ sufficiently small and apply Grönwall's inequality to obtain $\mathbf{u}(\cdot,\xi) = 0$ and $\int_0^\xi \theta(\cdot,t)\,\mathrm{d}t = 0$ a.e. in Ω for all $\xi \in (0,T)$. By differentiating the second equality with respect to ξ, it also follows that $\theta = 0$ a.e. in Q_T. Finally, from (24) we obtain that $\int_0^\eta h(t)\,\mathrm{d}t = 0$ for all $\eta \in (0,T)$ and by differentiating with respect to η, we may conclude that $h = 0$ a.e. in $(0,T)$. □

4. Existence of a solution: Dirichlet boundary condition for the temperature

In case of the Dirichlet boundary condition for the temperature, we propose the following linear recurrent scheme to approximate the original problem (7)–(9) for any $(\boldsymbol{\varphi},\psi) \in \mathbf{H}_0^1(\Omega)\times \mathrm{H}_0^1(\Omega)$ and $i = \overline{1,n}$:

$$
\rho\left(\delta^2\mathbf{u}_i, \boldsymbol{\varphi}\right) + \mu\left(\nabla\mathbf{u}_i, \nabla\boldsymbol{\varphi}\right) + (\lambda+\mu)\left(\nabla\cdot\mathbf{u}_i, \nabla\cdot\boldsymbol{\varphi}\right) + \beta\left(\nabla\theta_i, \boldsymbol{\varphi}\right) = \left(\mathbf{p}_i, \boldsymbol{\varphi}\right), \tag{26}
$$

$$
\rho C_s\left(\delta\theta_i, \psi\right) + \kappa\left(\nabla\theta_i, \nabla\psi\right) - T_0\beta\left(\delta\mathbf{u}_i, \nabla\psi\right) = h_i\left(f, \psi\right) + \left(F_i, \psi\right) - \left(\sum_{l=1}^{i} k_l\nabla\theta_{i-l}\tau, \nabla\psi\right), \tag{27}
$$

where

$$
h_i(f,\omega) = \rho C_s m_i' + \kappa\left(\nabla\theta_{i-1}, \nabla\omega\right) + \left(\sum_{l=1}^{i} k_l\nabla\theta_{i-l}\tau, \nabla\omega\right) - \beta T_0\left(\delta\mathbf{u}_{i-1}, \nabla\omega\right) - \left(F_i, \omega\right). \tag{28}
$$

The analysis is similar to that from Section 3. However, there is less work to be done since there are no boundary terms to handle in this case. We work now in the space $\mathbf{H}_0^1(\Omega)\times\mathrm{H}_0^1(\Omega)$, which is equipped with the norm $\left\|(\mathbf{u}\ \theta)^{\mathsf{T}}\right\|^2 = \|\nabla\mathbf{u}\|^2 + \|\nabla\theta\|^2$. We just state the existence result without a proof.

Theorem 4.1 (Existence and uniqueness: Dirichlet boundary condition). *Assume that* $\overline{\mathbf{u}}_0 \in \mathbf{H}_0^1(\Omega)$, $\overline{\mathbf{u}}_1 \in \mathbf{L}^2(\Omega)$, $\overline{\theta}_0 \in \mathrm{H}_0^1(\Omega)$, $f \in \mathrm{L}^2(\Omega)$ *with* $\int_\Omega f(\mathbf{x})\ \mathrm{d}\mathbf{x} \neq 0$, $m \in \mathrm{C}^1([0,T])$, $F \in \mathrm{L}^\infty\left((0,T), \mathrm{H}^1(\Omega)\right)$ *and*
$\mathbf{p} \in \mathrm{L}^\infty\left((0,T), \mathbf{H}^1(\Omega)\right)$. *Then there exists a unique triplet* $(\mathbf{u}, \theta, h)$ *that solves problem* (7)–(9) *such that*

- $\mathbf{u} \in \mathrm{C}\left([0,T], \mathbf{L}^2(\Omega)\right) \cap \mathrm{L}^2\left((0,T), \mathbf{H}_0^1(\Omega)\right)$,
  $\partial_t\mathbf{u} \in \mathrm{L}^2\left((0,T), \mathbf{L}^2(\Omega)\right) \cap \mathrm{C}\left([0,T], \mathbf{H}_0^1(\Omega)^*\right)$, $\partial_{tt}\mathbf{u} \in \mathrm{L}^2\left((0,T), \mathbf{H}_0^1(\Omega)^*\right)$;
- $\theta \in \mathrm{C}\left([0,T], \mathbf{L}^2(\Omega)\right) \cap \mathrm{L}^2\left((0,T), \mathrm{H}_0^1(\Omega)\right)$, $\partial_t\theta \in \mathrm{L}^2\left((0,T), \mathrm{H}_0^1(\Omega)^*\right)$;
- $h \in \mathrm{L}^2(0,T)$.

5. Numerical results and discussion

In the present numerical examples, we consider $k = 0$, i.e. type-I thermoelasticity. Firstly, we transform equations (1) in a dimensionless form by using the following non-dimensional variables, see e.g. [19, p. 388]:

$$\widetilde{\mathbf{x}} = \frac{1}{\ell}\mathbf{x}, \quad \widetilde{t} = \frac{C_1}{\ell}t, \quad \widetilde{\theta}(\widetilde{\mathbf{x}}, \widetilde{t}) = \frac{1}{T_0}\theta(\mathbf{x}, t), \quad \widetilde{\mathbf{u}}(\widetilde{\mathbf{x}}, \widetilde{t}) = \frac{\lambda + 2\mu}{\beta T_0 \ell}\mathbf{u}(\mathbf{x}, t), \quad \widetilde{g} = \frac{g}{T_0 \rho C_s C_1},$$
$$\widetilde{\mathbf{p}}(\widetilde{x}, \widetilde{t}) = \frac{\kappa}{\varrho\beta T_0 C_1 C_s}\mathbf{p}(x,t), \widetilde{h}(\widetilde{x}, \widetilde{t}) = \frac{\kappa}{\varrho^2 C_s^2 C_1^2 T_0}h(x,t), \quad \widetilde{m}(\widetilde{t}) = \frac{m(t)}{\ell T_0},$$

where $C_1 = \sqrt{(\lambda + 2\mu)/\rho}$ (SI unit: m/s) and $\ell = \kappa/(\rho C_s C_1)$ (SI unit: m). The inverse problem for the one-dimensional thermoelasticity system becomes (for simplicity, the tilde sign has been dropped in the following):

Find (u, θ, h) such that

$$\begin{cases} u_{tt}(x,t) - u_{xx}(x,t) + \theta_x(x,t) = p(x,t) & (x,t) \in (0,L) \times (0,T), \\ \theta_t(x,t) - \theta_{xx}(x,t) + \varepsilon_1 u_{xt}(x,t) = h(t)f(x) + F(x,t) & (x,t) \in (0,L) \times (0,T), \\ u(0,t) = u(L,t) = 0 & t \in (0,T], \\ \theta(0,t) = \theta(L,t) = 0 & \\ \ \text{or} \quad -\theta_x(L,t) = g(L,t),\ \theta_x(0,t) = g(0,t) & t \in (0,T], \\ u(x,0) = \overline{u}_0(x), \quad u_t(x,0) = \overline{u}_1(x), & x \in (0,L), \\ \theta(x,0) = \overline{\theta}_0(x), & x \in (0,L), \end{cases} \tag{29}$$

$$\int_0^L \omega(x)\theta(x,t) = m(t), \quad t \in [0,T], \tag{30}$$

where

$$\varepsilon_1 := \frac{\beta^2 T_0}{\varrho^2 C_s C_1^2}.$$

The two-dimensional linear model for an isotropic thermoelastic material is given by:

Find $(\mathbf{u}, \theta, h)$ such that

$$\begin{cases} \partial_{tt}\mathbf{u}(\mathbf{x},t) - \mu_1 \Delta \mathbf{u}(\mathbf{x},t) - (1-\mu_1)\nabla(\nabla \cdot \mathbf{u}(\mathbf{x},t)) + \nabla\theta(\mathbf{x},t) = \mathbf{p}(\mathbf{x},t), & (\mathbf{x},t) \in Q_T, \\ \theta_t(\mathbf{x},t) - \Delta\theta(\mathbf{x},t) + \varepsilon_1 \nabla \cdot \partial_t \mathbf{u}(\mathbf{x},t) = h(t)f(x) + F(\mathbf{x},t), & (\mathbf{x},t) \in Q_T, \\ \mathbf{u}(\mathbf{x},t) = \mathbf{0}, & (\mathbf{x},t) \in \Sigma_T, \\ \theta(\mathbf{x},t) = 0 \quad \text{or} \quad -\nabla\theta(\mathbf{x},t)\cdot\boldsymbol{\nu}(\mathbf{x}) = g(\mathbf{x},t) & (\mathbf{x},t) \in \Sigma_T, \\ \mathbf{u}(\mathbf{x},0) = \overline{\mathbf{u}}_0(\mathbf{x}), \quad \mathbf{u}_t(\mathbf{x},0) = \overline{\mathbf{u}}_1(\mathbf{x}), & \mathbf{x} \in \Omega, \\ \theta(\mathbf{x},0) = \overline{\theta}_0(\mathbf{x}), & \mathbf{x} \in \Omega \end{cases} \tag{31}$$

$$\int_\Omega \omega(x)\theta(x,t) = m(t), \quad t \in [0,T], \tag{32}$$

where

$$\mu_1 = \frac{\mu}{\lambda + 2\mu}.$$

The material constants employed in the numerical examples have been taken so that they correspond to a copper alloy [36], namely $G = 4.8\times10^{10}\, \mathrm{N/m^2}$, $\nu = 0.34$, $\alpha_T = 16.5\times10^{-6}\, \mathrm{1/K}$, $\kappa = 401\, \mathrm{W/mK}$, $\rho = 8960\, \mathrm{kg/m^3}$, $C_s = 385\, \mathrm{J/kgK}$ and $T_0 = 293\mathrm{K}$. Consequently, it follows that $\varepsilon_1 \approx 0.0189$ and $\mu_1 = 0.2424$.

The solution to the inverse source problems is found by applying the algorithm described by relations (10)–(12) in case of the Neumann boundary condition for the temperature and equations (26)–(28) when the Dirichlet boundary condition for the temperature is available. At each time step, the resulting elliptic mixed problems are solved numerically by the finite element method using the first-order (P1–FEM) Lagrange polynomials for the space discretization. More specifically, the finite element library DOLFIN [27, 28] from the FEniCS project [26, 1] has been employed herein.

The inherent errors present in real measurements have been simulated by adding to the measurement a randomly generated uncorrelated noise, namely

$$m_p(t) = m(t)\left(1 + p\mathcal{R}(t)\right), \qquad t \in \left\{ \frac{iT}{\widetilde{N}} : i = 0, \ldots, \widetilde{N} \right\},$$

where p represents the percentage of noise, e.g. $p = 0.01$ for 1% noise, and $\mathcal{R}$ is a Gaussian random variable of zero mean and standard deviation σ drawn from $[-1,1]$ that changes in time. We also note that the noise in the data can be estimated via the ordinary least-squares (OLS) method or the maximum likelihood estimation (MLE), see e.g. Rossi [37]. It has been assumed that $\widetilde{N} = 100$, i.e. the measurement is known at $(\widetilde{N}+1)$ time points. Then, the noisy data was regularized by using the nonlinear least-squares method to obtain a third-order polynomial approximating the noisy data for each noise level p. These polynomials have been used in the numerical examples presented and discussed in the following subsections.

5.1. One-dimensional problems in the two-dimensional setting

We consider $L = T = 1$ and prescribe the exact solution to problem (29)–(30) as follows

$$\begin{aligned} &u(x,t) = 0.1(1+t)^3 x(x-1)^2, && \theta(x,t) = 0.1(1+t)^2\sin(\pi x), \\ &h_1(t) = 1 - \exp(-t), && h_2(t) = \sin(2\pi t). \end{aligned} \tag{33}$$

We take $f(x) = \cos(x)$ and consider five different choices for the weight functions given by

$$\begin{aligned} \omega_1(x) &= \exp\left(-100x^2\right), \quad \omega_2(x) = \exp\left(-200x^2\right), \\ \omega_3(x) &= \exp\left(-400x^2\right), \quad \omega_4(x) = \exp\left(-100(x-0.6)^2\right), \\ \omega_5(x) &= \exp\left(-5000(x-0.6)^2\right). \end{aligned} \tag{34}$$

These weight functions are depicted in Figure 1 and define the position of the measurement. We note that ω_1, ω_2 and ω_3 are situated around $x = 0$ and these weight functions may be considered only in the case of Neumann boundary conditions since $\omega_j \notin \mathrm{H}^1_0(\Omega)$, $j = 1, 2, 3$. The time step for the equidistant time partitioning was chosen to be 10^{-3}, whilst the number of one-dimensional finite elements was taken to be equal to 200.

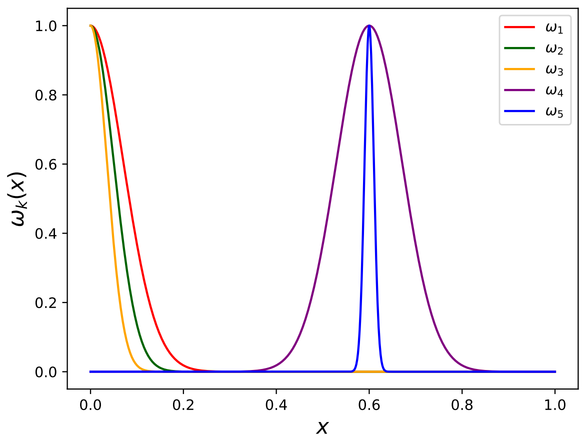

FIGURE 1. Weight functions used for Examples 1 and 2 (one dimension).

We further consider two numerical examples depending on whether the unknown source h_1 or h_2 is considered. For each example, both Neumann and Dirichlet boundary conditions for the temperature have been considered. It should be mentioned that the CPU time (Intel® Core^{TM} i7-8650U Processor) for one simulation (i.e. one level of noise p) was found to be around 10 s.

5.1.1. Example 1. First, we study the reconstruction of h_1 when either the Dirichlet or the Neumann boundary condition for the temperature is available, for the weight functions ω_i considered in equation (34). Figures 2–8 present the numerical solution in comparison with its exact value, as well as the corresponding absolute errors, obtained using various levels of noise added to the measurements.

The numerical results, retrieved using ω_4 and ω_5 and the Dirichlet boundary condition, are depicted in Figures 2 and 3, whilst Figures 7 and 8 show the numerical reconstructions, obtained yet again using ω_4 and ω_5 and the Neumann boundary condition. It can be seen from these figures that all of the numerical reconstructions for the source are good approximations for its exact counterpart and, at the same time, remain stable, whilst the best corresponding absolute errors are obtained for the Neumann boundary condition.

Good approximations for the source have also been obtained when considering the measurements corresponding to ω_1, ω_2 and ω_3 and these are presented in Figures 4-6, respectively. As expected, it can clearly be observed from these figures that the absolute errors in the numerically reconstructed sources increase as the support of the measurement becomes smaller.

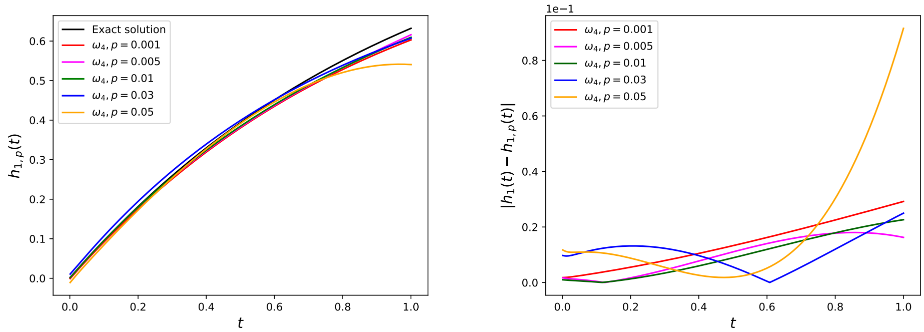

(a) (b)

FIGURE 2. Example 1 with Dirichlet boundary condition and ω_4: (a) The exact source and its numerical approximations, and (b) its corresponding absolute error, obtained for various levels of noise.

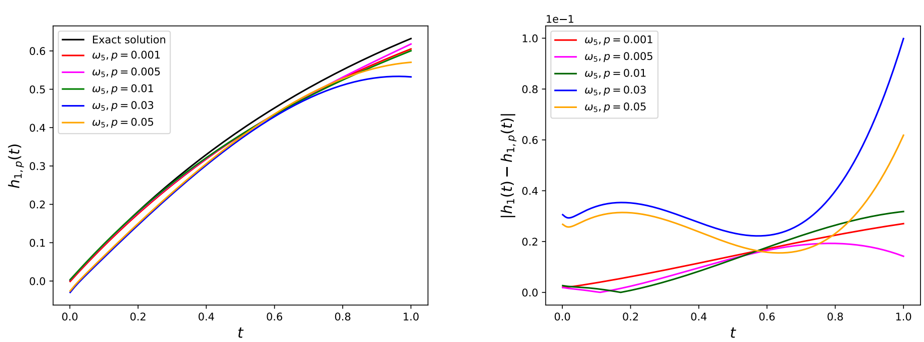

(a) (b)

FIGURE 3. Example 1 with Dirichlet boundary condition and ω_5: (a) The exact source and its numerical approximations, and (b) its corresponding absolute error, obtained for various levels of noise.

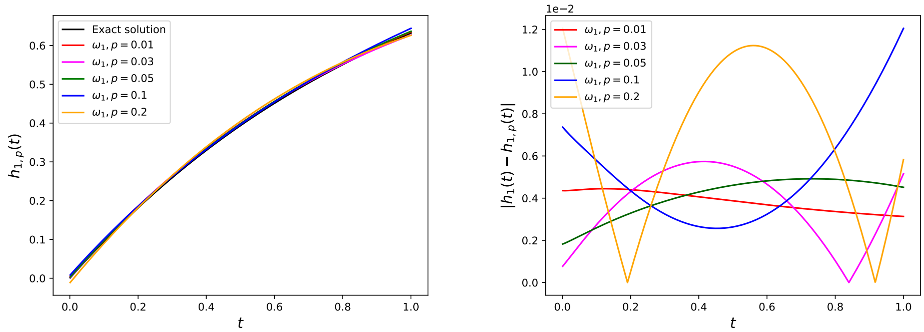

(a) (b)

FIGURE 4. Example 1 with Neumann boundary condition and ω_1: (a) The exact source and its numerical approximations, and (b) its corresponding absolute error, obtained for various levels of noise.

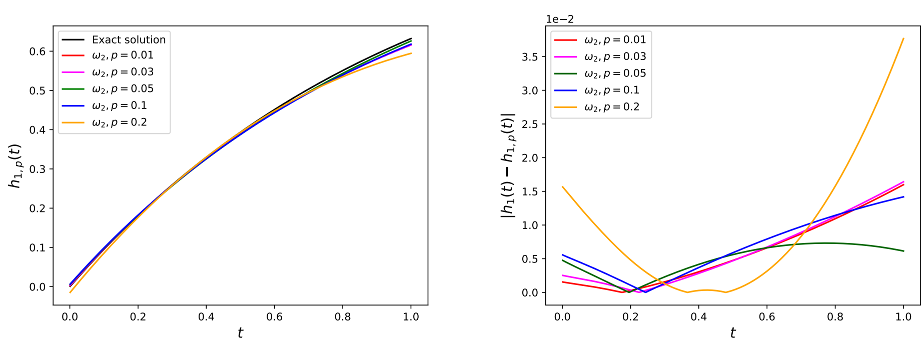

(a) (b)

FIGURE 5. Example 1 with Neumann boundary condition and ω_2: (a) The exact source and its numerical approximations, and (b) its corresponding absolute error, obtained for various levels of noise.

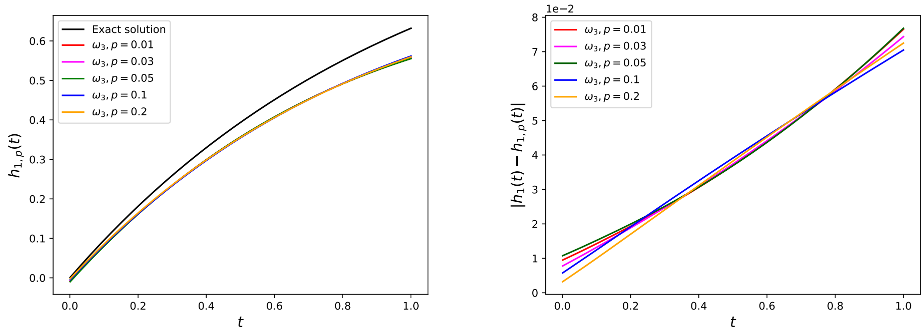

(a) (b)

FIGURE 6. Example 1 with Neumann boundary condition and ω_3: (a) The exact source and its numerical approximations, and (b) its corresponding absolute error, obtained for various levels of noise.

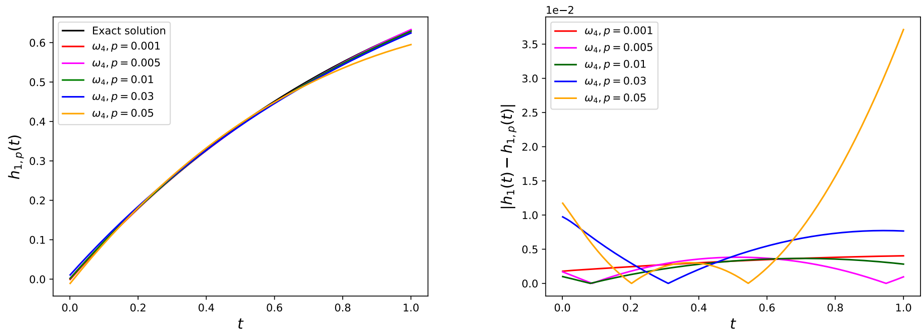

(a) (b)

FIGURE 7. Example 1 with Neumann boundary condition and ω_4: (a) The exact source and its numerical approximations, and (b) its corresponding absolute error, obtained for various levels of noise.

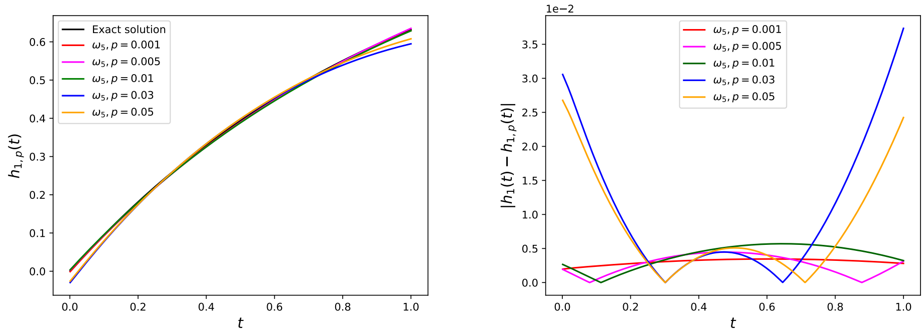

(a) (b)

FIGURE 8. Example 1 with Neumann boundary condition and ω_5: (a) The exact source and its numerical approximations, and (b) its corresponding absolute error, obtained for various levels of noise.

5.1.2. Example 2. In case of Example 2, we study the recovery of the sinusoidal source h_2 when either the Dirichlet or the Neumann boundary condition for the temperature is available. The numerical results for the source, obtained with various weight functions, are presented in Figures 9–15 and are similar to those retrieved for Example 1. From the numerical results presented in these figures, we may conclude that the algorithms described by relations (10)–(12) and (26)–(28), which correspond to Neumann and Dirichlet boundary conditions for the temperature, respectively, are stable with respect to decreasing the amount of noise added to the corresponding measurements.

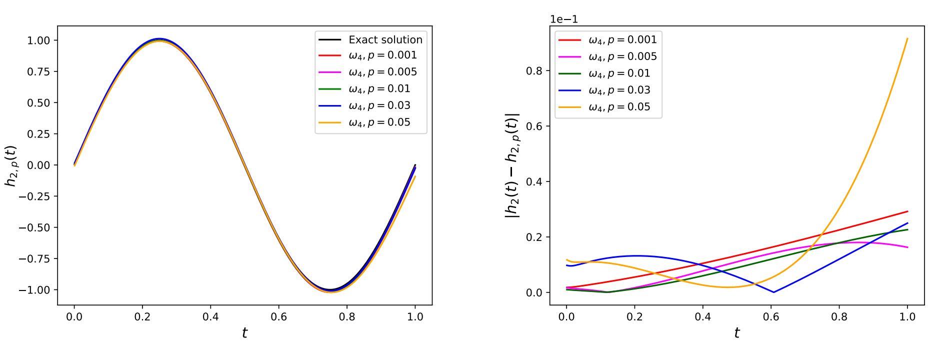

(a) (b)

FIGURE 9. Example 2 with Dirichlet boundary condition and ω_4: (a) The exact source and its numerical approximations, and (b) its corresponding absolute error, obtained for various levels of noise.

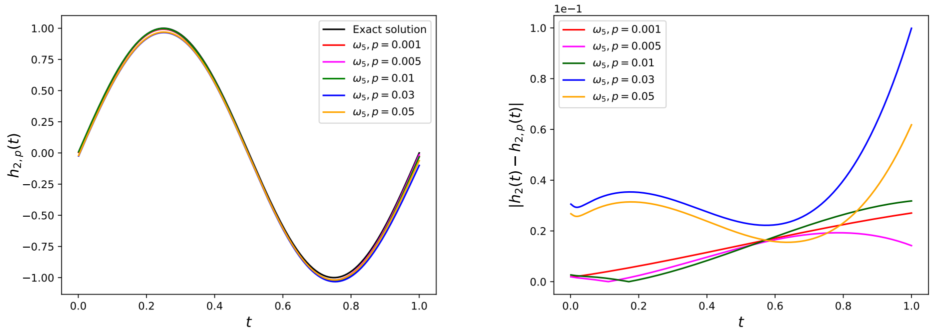

(a) (b)

FIGURE 10. Example 2 with Dirichlet boundary condition and ω_5: (a) The exact source and its numerical approximations, and (b) its corresponding absolute error, obtained for various levels of noise.

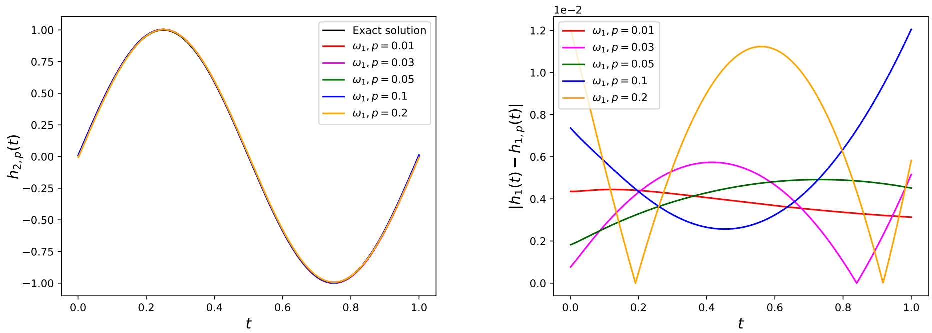

(a) (b)

FIGURE 11. Example 2 with Neumann boundary condition and ω_1: (a) The exact source and its numerical approximations, and (b) its corresponding absolute error, obtained for various levels of noise.

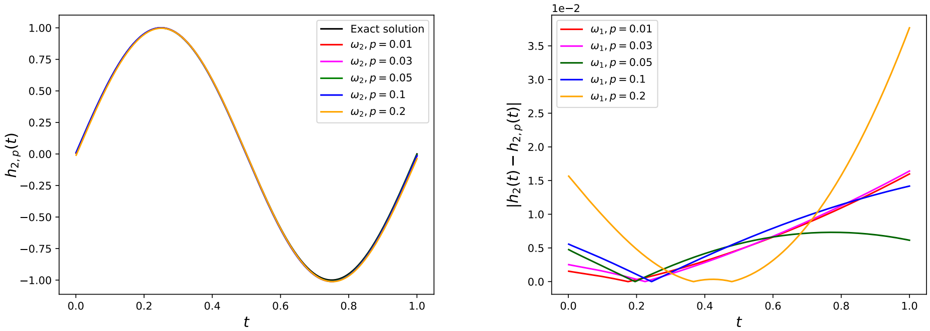

(a) (b)

FIGURE 12. Example 2 with Neumann boundary condition and ω_2: (a) The exact source and its numerical approximations, and (b) its corresponding absolute error, obtained for various levels of noise.

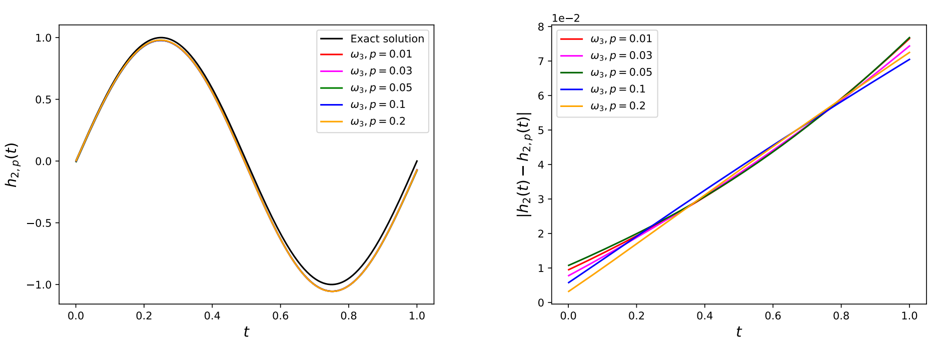

(a) (b)

FIGURE 13. Example 2 with Neumann boundary condition and ω_3: (a) The exact source and its numerical approximations, and (b) its corresponding absolute error, obtained for various levels of noise.

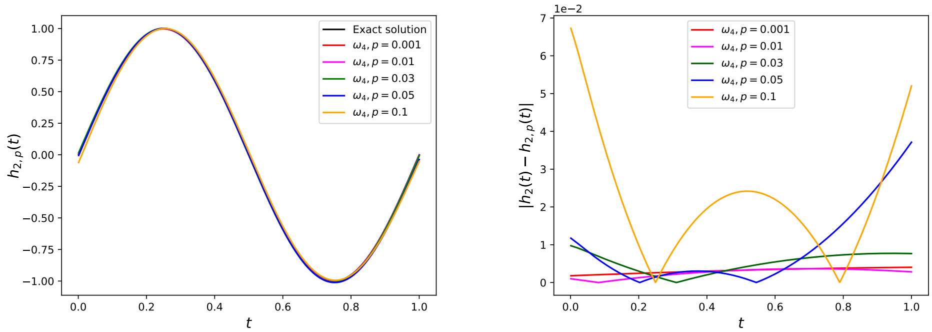

(a) (b)

FIGURE 14. Example 2 with Neumann boundary condition and ω_4: (a) The exact source and its numerical approximations, and (b) its corresponding absolute error, obtained for various levels of noise.

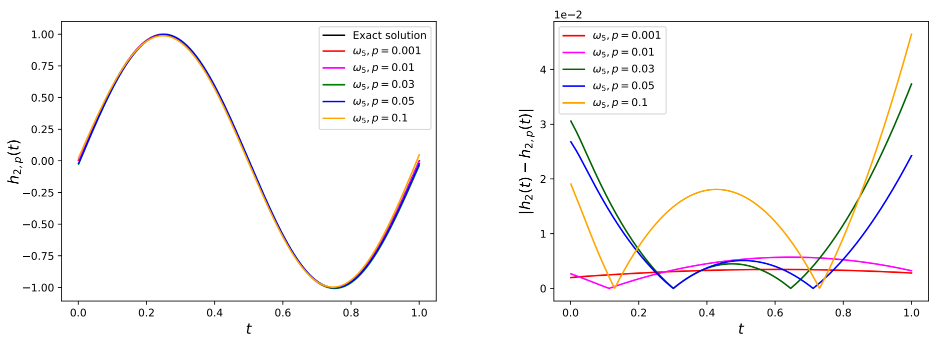

(a) (b)

FIGURE 15. Example 2 with Neumann boundary condition and ω_5: (a) The exact source and its numerical approximations, and (b) its corresponding absolute error, obtained for various levels of noise.

5.2. Two-dimensional problems in the three-dimensional setting

The data for the numerical example are derived from the following exact solution to problem (31)–(32), which is chosen according to [30, Proposition 1]:

$$
\begin{aligned}
&\mathbf{u}(x,y,t) = (1+t)^3 \frac{C_d}{2} \left[\ln\left((x+5)^2 + (y+1)^2\right)(x+5), \ln\left((x+5)^2 + (y+1)^2\right)(y+1) \right]^{\mathsf{T}}, \\
&\theta(x,y,t) = \frac{1}{2}(1+t)^2 \ln\left((x+5)^2 + (y+1)^2\right), \\
&h_1(t) = 1 - \exp(-t), \quad h_2(t) = \sin(2\pi t), \\
&f(x,y) = \cos(xy), \quad \omega(x,y) = \exp\left(1 - \frac{0.5^2}{0.5^2 - (0.5-x)^2} - \frac{0.5^2}{0.5^2 - (0.5-y)^2}\right),
\end{aligned}
$$

where

$$
C_d \coloneqq \frac{\alpha_T}{2} \left(\frac{1+\nu}{1-\nu} \right) \approx 1.68 \times 10^{-5}.
$$

The time step for the two-dimensional examples investigated herein, i.e. Examples 3 and 4, was chosen to be 10^{-3}, whilst the number of two-dimensional finite elements was taken to be equal to 5000. The weight function employed in case of Examples 3 and 4 is presented in Figure 16.

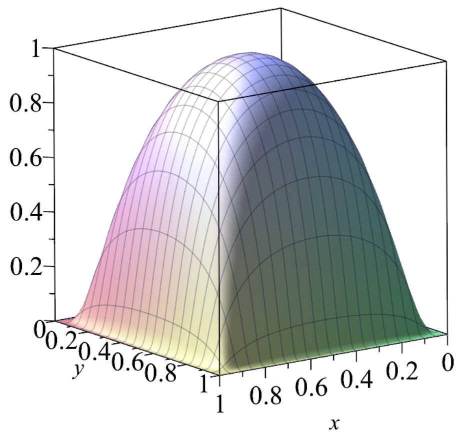

FIGURE 16. Weight function used for Examples 3 and 4 (two dimensions).

Further, we also consider two examples corresponding to the numerical reconstruction of the unknown sources h_1 and h_2, respectively. The CPU time for one simulation (i.e. one level of noise) was found to be around 25 min.

5.2.1. Example 3. Figure 17 displays the results for the reconstruction of the heat source h_1, retrieved using the Dirichlet boundary condition for the temperature and various levels of noise added to the measurement, in comparison with its exact value. Despite the complexity of this inverse problem, it can be seen from this figure that the numerical approximations for the heat source h_1 are stable with respect to the level of noise added to the measured data and an accurate numerical result for h_1 is obtained for a low amount of noise $p < 0.005$.

We also note that similar results have been obtained in case of the Neumann boundary condition for the temperature, see Figure 18. Analogous to the numerical reconstructions retrieved for the one-dimensional Examples 1 and 2, the numerically reconstructed heat sources in case of the Neumann conditions for the temperature are more inaccurate that those corresponding to the Dirichlet boundary condition for the temperature, for Example 3, see Figures 17 and 18.

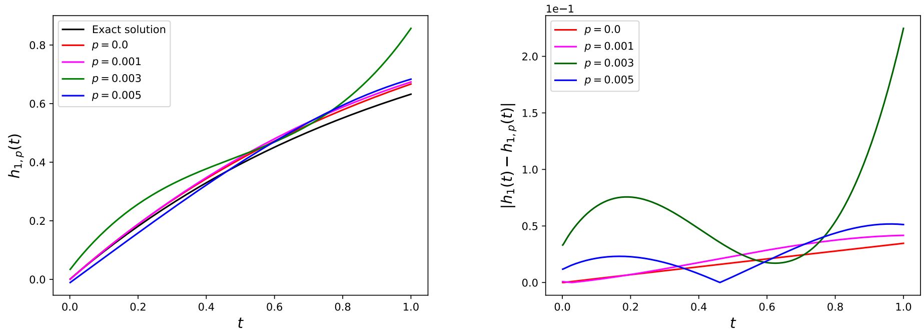

(a) (b)

FIGURE 17. Example 3 with Dirichlet boundary condition: (a) The exact source and its numerical approximations, and (b) its corresponding absolute error, obtained for various levels of noise.

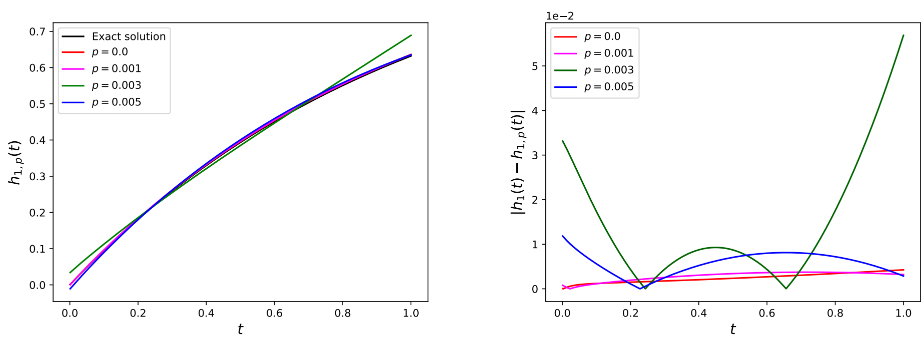

(a) (b)

FIGURE 18. Example 3 with Neumann boundary conditions: (a) The exact source and its numerical approximations, and (b) its corresponding absolute error, obtained for various levels of noise.

5.2.2. Example 4. The exact and numerical results for the sinusoidal heat source h_2, obtained using various levels of noise added to the measurement in case of the Dirichlet and the Neumann boundary conditions for the temperature, as well as the corresponding absolute errors are illustrated in Figures 19 and 20, respectively. Yet again, we may conclude that the numerical approximations for the heat source h_2 are stable with respect to decreasing the amount of noise added to the measurement, whilst the accuracy of the numerically reconstructed heat source is good in case of a low level of noise.

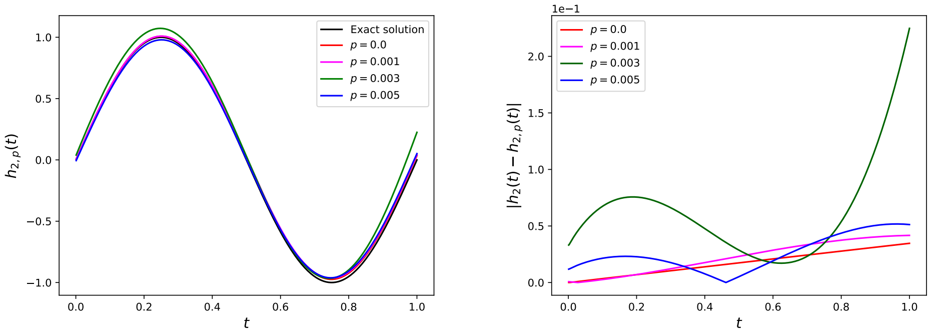

(a) (b)

FIGURE 19. Example 4 with Dirichlet boundary condition: (a) The exact source and its numerical approximations, and (b) its corresponding absolute error, obtained for various levels of noise.

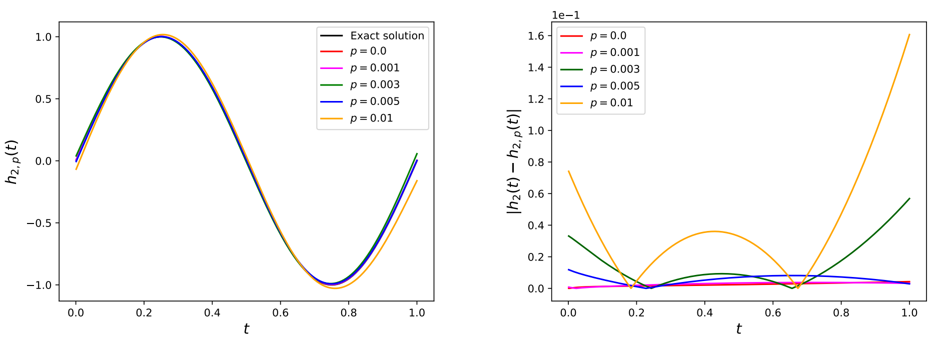

(a) (b)

FIGURE 20. Example 4 with Neumann boundary condition: (a) The exact source and its numerical approximations, and (b) its corresponding absolute error, obtained for various levels of noise.

6. Conclusions

In this paper, an inverse source problem for the isotropic thermoelasticity system of type-III has been investigated. In particular, both the theoretical and the numerical reconstructions of a solely time-dependent heat source from a weighted integral measurement of the temperature have been studied. Firstly, the inverse problem was reformulated as a coupled direct problem. A clear distinction has been made between the Neumann and the Dirichlet boundary conditions for the temperature and this has led to different conditions on the weight function in the measurement. In each case, a convergent and stable algorithm, based on Rothe's method and built on a decoupling technique, has been proposed for the recovery of the missing source. The existence and uniqueness of a weak solution to the problem has also been proved. Four numerical examples (two in one dimension and another two in two dimensions) corresponding to a copper alloy have been implemented using the finite element method, with the mention that the noisy data was regularized. The numerical results obtained for these examples have validated both the convergence and the stability of the proposed algorithms.

Future work will be concerned with the investigation of this inverse problem by employing a different technique, such as the Tikhonov regularization method, as well as the study of the recovery of a heat source in the dual-phase lag theory of thermoelasticity.

Acknowledgements. Karel Van Bockstal was supported by a postdoctoral fellowship of the Research Foundation - Flanders (106016/12P2919N). The work of Liviu Marin was supported by a grant of the Romanian Ministry of Research and Innovation, CNCS–UEFISCDI, project number PN–III–P1–1.1–TE–2019–0348, within PNCDI III.

Conflict of interest

The authors declare that they have no conflict of interest.

References

[1] Alnæs, M.S., Blechta, J., Hake, J., Johansson, A., Kehlet, B., Logg, A., Richardson, C., Ring, J., Rognes, M.E., Wells, G.N.: The FEniCS project version 1.5. Archive of Numerical Software **3**(100), 9–23 (2015)

[2] Bellassoued, M., Yamamoto, M.: Carleman estimates and an inverse heat source problem for the thermoelasticity system. Inverse Problems **27**(1), 015006 (2011)

[3] Bermúdez, A., Viaño, J.M.: Étude de deux schémas numériques pour les équations de la thermoélasticité (study of two numerical schemes for the equations of thermoelasticity). RAIRO Anal. Numér. **17**(2), 121–136 (1983)

[4] Biot, M.A.: Thermoelasticity and irreversible thermodynamics. J. Appl. Phys. **27**(3), 240–253 (1956)

[5] Cannon, J.R., Lin, Y.: Determination of a parameter p(t) in some quasi-linear parabolic differential equations. Inverse Problems **4**(1), 35–45 (1988)

[6] Chou, S.I., Wang, C.C.: Estimates of error in finite element approximate solutions to problems in linear thermoelasticity. I. Computationally coupled numerical schemes. Arch. Rational Mech. Anal. **77**(3), 263–299 (1981)

[7] Ciarlet, P.G.: Linear and Nonlinear Functional Analysis with Applications. Applied mathematics. Society for Industrial and Applied Mathematics (2013). URL `https://books.google.be/books?id=AUlWAQAAQBAJ`

[8] Dafermos, C.M.: On the existence and the asymptotic stability of solutions to the equations of linear thermoelasticity. Arch. Rational Mech. Anal. **29**, 241–271 (1968)

[9] Dennis, B.H., Dulikravich, G.S.: Simultaneous determination of temperatures, heat fluxes, deformations, and tractions on inaccessible boundaries. Journal of Heat Transfer **121**(3), 537–545 (1999)

[10] Dennis, B.H., Jin, W., Dulikravich, G.S., J., J.: Application of the Finite Element Method to Inverse Problems in Solid Mechanics. International Journal of Structural Changes in Solids **3**(2), 11–21 (2011)

[11] Dennis, B.H., Yoshimura, S., Dulikravich, G.S.: A Finite Element Formulation for the Determination of Unknown Boundary Conditions for 3-D Steady Thermoelastic Problems. ASME Journal of Heat Transfer **126**, 110–118 (2004)

[12] Duvaut, G., Lions, J.L.: Inéquations en thermoélasticité et magnétohydrodynamique (inequalities in thermoelasticity and magnetohydrodynamic). Arch. Rational Mech. Anal. **46**, 241–279 (1972)

[13] Green, A.E., Naghdi, P.M.: A re-examination of the basic postulates of themomechanics. Proc. Royal Society London A **432**(1885), 171–194 (1991)

[14] Grimmonprez, M., Marin, L., Van Bockstal, K.: The reconstruction of a solely time-dependent load in a simply supported non-homogeneous Euler–Bernoulli beam. Applied Mathematical Modelling **79**, 914–933 (2020)

[15] Grimmonprez, M., Slodička, M.: Reconstruction of an unknown source parameter in a semilinear parabolic problem. J. Comput. Appl. Math. **289**, 331–345 (2015)

[16] Gurtin, M.E.: The linear theory of elasticity. Encyclopedia of Physics, Vol. VIa/2: Mechanics of Solids. Springer-Verlag, Berlin (1972)

[17] Hadamard, J.: Lectures on Cauchy Problem in Linear Partial Differential Equations. Yale University Press, New Haven (1923)

[18] Hazanee, A., Ismailov, M., Lesnic, D., Kerimov, N.: An inverse time-dependent source problem for the heat equation. Applied Numerical Mathematics **69**(0), 13 – 33 (2013)

[19] Hetnarski, R.B., Eslami, M.R.: Thermal stresses – advanced theory and applications., vol. 158. Dordrecht: Springer (2009)

[20] Hu, W., Gu, Y., Zhang, C., He, X.: The generalized finite difference method for an inverse boundary value problem in three-dimensional thermo-elasticity. Advances in Engineering Software **131**, 1–11 (2019)

[21] Ikehata, M.: On finding a cavity in a thermoelastic body using a single displacement measurement over a finite time interval on the surface of the body. J. Inverse Ill-Posed Probl. **26**(3), 369–394 (2018)

[22] Ismailov, M., Kanca, F., Lesnic, D.: Determination of a time-dependent heat source under nonlocal boundary and integral overdetermination conditions. Appl. Math. Comput. **218**(8), 4138–4146 (2011)

[23] Kačur, J., Ženíšek, A.: Analysis of approximate solutions of coupled dynamical thermoelasticity and related problems. Apl. Mat. **31**(3), 190–223 (1986)

[24] Karageorghis, A., Lesnic, D., Marin, L.: The method of fundamental solutions for an inverse boundary value problem in static thermo-elasticity. Computers & Structures **135**, 32–39 (2014)

[25] Kačur, J.: Method of Rothe in evolution equations, *Teubner Texte zur Mathematik*, vol. 80. Teubner, Leipzig (1985)

[26] Logg, A., Mardal, K.A., Wells, G.N., et al.: Automated Solution of Differential Equations by the Finite Element Method. Springer, Berlin, Heidelberg (2012)

[27] Logg, A., Wells, G.N.: DOLFIN: Automated Finite Element Computing. ACM Trans. Math. Software **37**(2), 28 (2010)

[28] Logg, A., Wells, G.N., Hake, J.: DOLFIN: a C++/Python Finite Element Library, chap. 10. Springer, Berlin, Heidelberg (2012)

[29] Marin, L., Karageorghis, A.: The MFS for the Cauchy problem in two-dimensional steady-state linear thermoelasticity. International Journal of Solids and Structures **50**(20–21), 3387–3398 (2013)

[30] Marin, L., Karageorghis, A., Lesnic, D.: A numerical study of the SVD–MFS solution of inverse boundary value problems in two-dimensional steady-state linear thermoelasticity. Numerical Methods for Partial Differential Equations **31**(1), 168–201 (2015)

[31] Marin, L., Karageorghis, A., Lesnic, D.: Regularized MFS solution of inverse boundary value problems in three-dimensional steady-state linear thermoelasticity. International Journal of Solids and Structures **91**, 127–142 (2016)

[32] Nedin, R., Nesterov, S., Vatulyan, A.: On an inverse problem for inhomogeneous thermoelastic rod. International Journal of Solids and Structures **51**(3–4), 767–773 (2014)

[33] Nickell, R.E., Sackman, J.L.: Approximate solutions in linear, coupled thermoelasticity. J. Appl. Mech. **35**, 255–266 (1968)

[34] Nickell, R.E., Sackman, J.L.: Variational principles for linear coupled thermoelasticity. Quart. Appl. Math. **26**, 11–26 (1968)

[35] Prilepko, A.I., Orlovsky, D.G., Vasin, I.A.: Methods for Solving Inverse Problems in Mathematical Physics. Chapman & Hall/CRC Pure and Applied Mathematics. Taylor & Francis (2000)

[36] Ross, R.: Metallic materials specification handbook. Spon (1980). URL `https://books.google.be/books?id=XORRAAAAMAAJ`

[37] Rossi, J.D.: Mathematical Statistics: An Introduction to Likelihood Statistical Inference. John Wiley & Sons, Hoboken, NJ, USA (2018)

[38] Slodička, M.: Determination of a solely time-dependent source in a semilinear parabolic problem by means of boundary measurements. Journal of Computational and Applied Mathematics **289**, 433–440 (2015)

[39] Van Bockstal, K.: Numerical techniques for partial differential equations in superconductivity and thermoelasticity. Ph.D. thesis, Ghent University, Ghent (2015)

[40] Van Bockstal, K., Marin, L.: Recovery of a space-dependent vector source in anisotropic thermoelastic systems. Computer Methods in Applied Mechanics and Engineering **321**, 269–293 (2017)

[41] Van Bockstal, K., Slodička, M.: Recovery of a space-dependent vector source in thermoelastic systems. Inverse Problems Sci. Eng. **23**(6), 956–968 (2015)

[42] Van Bockstal, K., Slodička, M.: Recovery of a time-dependent heat source in one-dimensional thermoelasticity of type-III. Inverse Problems in Science and Engineering **25**(5), 749–770 (2017)

[43] Wu, B., Liu, J.: Determination of an unknown source for a thermoelastic system with a memory effect. Inverse Problems **28**(9), 095012 (2012)

[44] Wu, B., Yu, J., Wang, Z.: Uniqueness and stability of an inverse kernel problem for type-III thermoelasticity. J. Math. Anal. and Appl. **402**(1), 242–254 (2013)

[45] Xu, Y.: An inverse problem for the quasistatic thermoelastic system on the unit disk. Applicable Analysis **73**(1–2), 295–305 (1999)

[46] Ženíšek, A.: Finite element methods for coupled thermoelasticity and coupled consolidation of clay. RAIRO Anal. Numér. **18**(2), 183–205 (1984)

Karel Van Bockstal
Research Group NaM^2, Department of Electronics and Information systems, Ghent University, Krijgslaan 281, 9000 Ghent, Belgium
e-mail: `Karel.VanBockstal@UGent.be,karelvanbockstal@gmail.com`

Liviu Marin
Department of Mathematics, Faculty of Mathematics and Computer Science, University of Bucharest, 14 Academiei, 010014 Bucharest, Romania
"Gheorghe Mihoc – Caius Iacob" Institute of Mathematical Statistics and Applied Mathematics of the Romanian Academy, 13 Calea 13 Septembrie, 050711 Bucharest, Romania
e-mail: `liviu.marin@fmi.unibuc.ro,marin.liviu@gmail.com`